TABLE 2. Association results between 15 SNPs in 10 candidate loci and type 2 diabetes in Japanese

		Dominant model					Recessive model				
					95% CI					95% CI	
Gene	SNP ID	*P* value	*P* value[a]	OR	Lower	Upper	*P* value	*P* value[a]	OR	Lower	Upper
SLC30A8	rs13266634	0.063	0.24	1.17	0.99	1.39	5.8×10^{-3}	0.074	1.22	1.06	1.40
SLC30A8	rs3802177	0.15	0.36	1.14	0.95	1.36	1.3×10^{-3}	0.020	1.27	1.10	1.46
HHEX	rs1111875	6.4×10^{-5}	1.6×10^{-5}	1.32	1.15[a]	1.51	3.5×10^{-3}	0.083	1.40	1.12	1.77
HHEX	rs7923837	1.8×10^{-4}	1.9×10^{-3}	1.31	1.14[a]	1.50	0.036	0.15	1.42	1.02	1.97
LOC387761	rs7480010	0.37	0.16	1.17	0.83[a]	1.65	0.44	0.28	1.06	0.92	1.22
EXT2	rs3740878	0.99	0.66	1.00	0.87[a]	1.15	0.49	0.50	1.07	0.88	1.30
CDKN2B	rs10811661	4.0×10^{-5}	2.3×10^{-5}	1.44	1.21[a]	1.72	1.9×10^{-4}	1.8×10^{-4}	1.31	1.14	1.51
CDKN2B	rs564398	0.88	0.51	1.03	0.68[a]	1.58	0.66	0.65	1.03	0.89	1.20
GCKR	rs7800944	0.14	0.34	1.12	0.96[a]	1.29	0.033	4.2×10^{-3}	1.20	1.01	1.41
Inter gene	rs9300039	0.098	0.20	1.26	0.96[a]	1.66	0.85	0.32	1.01	0.88	1.16
IGF2BP2	rs4402960	9.5×10^{-4}	0.018	1.26	1.10[a]	1.44	1.7×10^{-3}	4.9×10^{-4}	1.42	1.14	1.77
IGF2BP2	rs1470579	0.014	0.063	1.18	1.03[a]	1.36	1.6×10^{-3}	9.2×10^{-4}	1.40	1.13	1.72
CDKAL1	rs7754840	1.6×10^{-3}	1.6×10^{-3}	1.26	1.09[a]	1.46	1.3×10^{-7}	1.5×10^{-7}	1.58	1.33	1.87
CDKAL1	rs7756992	0.01	0.022	1.22	1.05[a]	1.42	4.2×10^{-8}	7.4×10^{-7}	1.55	1.32	1.82
FTO	rs9939609	0.98	0.60	1.00	0.87[a]	1.15	0.28	0.70	1.20	0.86	1.67

ORs, 95% CIs, and *P* values under a dominant or recessive model of each risk allele are given for 15 SNPs identified in French, decode, Diabetes Genetics Initiative, Wellcome Trust Case Control Consortium, and Finland-United States Investigation of Noninsulin-Dependent Diabetes Mellitus Genetics studies. ID, Identification.

[a] *P* values adjusted for age, sex, and BMI.

was found only in control subjects. In addition, subjects with the risk A allele tended to show a larger BMI, as previously reported in Caucasians (13), although it did not reach the level of statistical significance. The mean values of BMI were 22.4 ± 3.2 (TT) and 22.7 ± 3.1 kg/m^2 (AA + AT) for controls ($P = 0.051$). On the other hand, these values were 23.6 ± 3.4 (TT) and 23.8 ± 3.8 kg/m^2 (AA + AT) for cases ($P = 0.306$). Although *HHEX*, *CDKN2B*, *IGF2BP2*, and *CDKAL1* were associated with pancreatic β-cell function in recent reports (15–17), we failed to detect an association with HOMA-β in this study. There was also no evidence of association between HOMA-IR and the risk alleles of these genes.

Discussion

Recent reports have revealed novel type 2 diabetes-susceptibility genes such as *SLC30A8*, *HHEX*, *CDKN2B*, *IGF2BP2*, and *CDKAL1* in the European population (8, 9, 11, 12). In addition, *FTO* and *GCKR* were associated with BMI and serum TG level, respectively (10, 13). In this study we confirmed that all of the proven genes found in Caucasians are replicated in Japanese. The strongest association by *P* value at the 10^{-6}–10^{-7} level was found at *CDKN2B* (rs10811661) and *CDKAL1* (rs7754840, rs7756992), followed by *HHEX* (rs1111875, rs7923837) and *IGF2BP2* (rs4402960, rs1470579). The odds ratio (OR) values of the first three SNPs were 1.27, 1.28, and 1.27, respectively, an even stronger association than that found in the original genome-wide association study in Europeans (10, 14). There were considerable differences in the frequencies of the risk alleles (Table 1), resulting in difficulty of replication due to decreased power of the study in addition to that due to population difference. According to the previous report in Japanese, the SNPs in *HHEX* showed the strongest association with type 2 diabetes, although the frequencies of risk alleles of SNPs in *HHEX* were even lower in the Japanese samples than European populations (15, 18). The previous report showed significant association with both SNPs in *HHEX* but not with the SNPs in *IGF2BP2* (15). This discrepancy cannot be explained by the small sample number because the risk allele frequencies of *IGF2BP2* are higher in Japanese than Europeans, in contrast to those of *HHEX*.

Although the previous study did not detect association of *IGF2BP2* with type 2 diabetes (15), the gene was detected as a diabetes-susceptibility gene in the present study. The absence of significant association in the previous study may be due to the lack of power deriving mainly from the small sample number. Recently, another study in Japanese has reported that rs4402960 in *IGF2BP2* showed the strongest association with type 2 diabetes, using a larger number of samples (19). The present study had 86% power to detect an OR of 1.20 when the frequency of a risk allele was 35% (rs4402960) and the *P* value was less than 0.0033. However, it is important to note that association study is dependent on discrimination of case and control subjects. It also has been reported that lifestyle changes can reduce the risk of type 2 diabetes, even in individuals carrying the type 2 diabetes-susceptibility variant of *TCF7L2* (20).

CDKAL1 and *CDKN2B* showed a nominal association with type 2 diabetes in a previous report in Japanese (15, 19). SNP rs7756992 in *CDKAL1* has been associated with type 2 diabetes in Han Chinese individuals from Hong Kong (12). A strong association between this SNP and type 2 diabetes [OR = 1.27 (95% confidence interval (CI) 1.15–1.40); $P = 9.8 \times 10^{-7}$] was detected in this study. Because type 2 diabetes in Asians is characterized primarily by β-cell dysfunction, these two genes might well be involved in transduction of glucose toxicity or regenerative capacity of pancreatic β-cells and, thus, are possible susceptibility genes for Japanese type 2 diabetes.

We found a nominal association of *GCKR* (rs780094) with the serum TG level both in case and control subjects, as previously reported in Caucasians (10). A nominal association of the

SNP of *FTO* (rs9939609) with BMI was found only in control subjects. In addition, the subjects with risk A allele showed somewhat larger BMI values, as has been reported in Caucasians (13). *FTO* was identified as a type 2 diabetes-susceptibility variant that predisposes to diabetes in the United Kingdom population through its effect on BMI. The lack of association between BMI and the *FTO* SNPs in Japanese could be due to the fact that our samples were from a less obese population.

In conclusion, we were able to replicate a significant association with the largest number of samples so far in Japanese between type 2 diabetes and SNPs in *SLC30A*, *HHEX*, *CDKN2B*, *IGF2BP2*, and *CDKAL1*, which suggests that these variants represent common type 2 diabetes-susceptibility genes in both Japanese and Europeans. Further investigation is required to identify the most likely functional variants.

Acknowledgments

We thank Drs. Hideichi Makino, Kishio Nanjo, Takashi Kadowaki, Kazuo Hara, Haruhiko Osawa, Hiroto Furuta, Sumio Sugano, and Shoji Tsuji for their contributions and helpful discussion throughout the project.

Address all correspondence and requests for reprints to: Masato Kasuga, Division of Diabetes, Metabolism and Endocrinology, Department of Internal Medicine, Kobe University Graduate School of Medicine, 7-5-1 Kusunoki-cho, Chuo-ku, Kobe 650-0017, Japan. E-mail: kasuga@med.kobe-u.ac.jp.

This work was supported by Grant-in-Aid for Scientific Research on Priority Areas (C), "Medical Genome Science (Millennium Genome Project)," "Applied Genomics," and "Comprehensive Genomics" by the Ministry of Education, Culture, Sports, Science, and Technology of Japan, and in part by a New Energy and Industrial Technology Development Organization grant (to Y.Ho.).

Present address for K.Yamag.: Department of Medical Biochemistry Faculty of Medical and Pharmaceutical Sciences, Kumamoto University, Kumamoto 860-8556, Japan.

Present address for Y.Y.: Department of Internal Medicine, Akita University School of Medicine, Akita 010-8543, Japan.

Present address for Y.S.: Kansai Electric Power Hospital, Osaka 553-0003, Japan.

Disclosure Statement: The authors have nothing to disclose.

References

1. Grant SF, Thorleifsson G, Reynisdottir I, Benediktsson R, Manolescu A, Sainz J, Helgason A, Stefansson H, Emilsson V, Helgadottir A, Styrkarsdottir U, Magnusson KP, Walters GB, Palsdottir E, Jonsdottir T, Gudmundsdottir T, Gylfason A, Saemundsdottir J, Wilensky RL, Reilly MP, Rader DJ, Bagger Y, Christiansen C, Gudnason V, Sigurdsson G, Thorsteinsdottir U, Gulcher JR, Kong A, Stefansson K 2006 Variant of transcription factor 7-like 2 (*TCF7L2*) gene confers risk of type 2 diabetes. Nat Genet 38:320–323
2. Groves CJ, Zeggini E, Minton J, Frayling TM, Weedon MN, Rayner NW, Hitman GA, Walker M, Wiltshire S, Hattersley AT, McCarthy MI 2006 Association analysis of 6,736 U.K. subjects provides replication and confirms *TCF7L2* as a type 2 diabetes susceptibility gene with a substantial effect on individual risk. Diabetes 55:2640–2644
3. Zhang C, Qi L, Hunter DJ, Meigs JB, Manson JE, van Dam RM, Hu FB 2006 Variant of transcription factor 7-like 2 (*TCF7L2*) gene and the risk of type 2 diabetes in large cohorts of U.S. women and men. Diabetes 55:2645–2648
4. Scott LJ, Bonnycastle LL, Willer CJ, Sprau AG, Jackson AU, Narisu N, Duren WL, Chines PS, Stringham HM, Erdos MR, Valle TT, Tuomilehto J, Bergman RN, Mohlke KL, Collins FS, Boehnke M 2006 Association of transcription factor 7-like 2 (*TCF7L2*) variants with type 2 diabetes in a Finnish sample. Diabetes 55:2649–2653
5. Cauchi S, Meyre D, Dina C, Choquet H, Samson C, Gallina S, Balkau B, Charpentier G, Pattou F, Stetsyuk V, Scharfmann R, Staels B, Frühbeck G, Froguel P 2006 Transcription factor *TCF7L2* genetic study in the French population: expression in human beta-cells and adipose tissue and strong association with type 2 diabetes. Diabetes 55:2903–2908
6. Miyake K, Horikawa Y, Hara k, Yasuda k, Osawa H, Furuta H, Hirota Y, Yamagata K, Hinokio Y, Oka Y, Iwasaki N, Iwamoto Y, Yamada Y, Seino Y, Maegawa H, Kashiwagi A, Yamamoto K, Tokunaga K, Takeda J, Makino H, Nanjo K, Kadowaki K, Kasuga M 2008 Association of *TCF7L2* polymorphisms with susceptibility to type 2 diabetes in 4,087 Japanese subjects. J Hum Genet 53:174–180
7. Guo T, Hanson RL, Traurig M, Muller YL, Ma L, Mack J, Kobes S, Knowler WC, Bogardus C, Baier LJ 2007 TCF7L2 is not a major susceptibility gene for type 2 diabetes in Pima Indians: analysis of 3,501 individuals. Diabetes 56: 3082–3088
8. The Wellcome Trust Case Control Consortium 2007 Genome-wide association study of 14,000 cases of seven common diseases and 3,000 shared controls. Nature 447:661–678
9. Scott LJ, Mohlke KL, Bonnycastle LL, Willer CJ, Li Y, Duren WL, Erdos MR, Stringham HM, Chines PS, Jackson AU, Prokunina-Olsson L, Ding CJ, Swift AJ, Narisu N, Hu T, Pruim R, Xiao R, Li XY, Conneely KN, Riebow NL, Sprau AG, Tong M, White PP, Hetrick KN, Barnhart MW, Bark CW, Goldstein JL, Watkins L, Xiang F, Saramies J, Buchanan TA, Watanabe RM, Valle TT, Kinnunen L, Abecasis GR, Pugh EW, Doheny KF, Bergman RN, Tuomilehto J, Collins FS, Boehnke M 2007 A genome-wide association study of type 2 diabetes in Finns detects multiple susceptibility variants. Science 316: 1341–1345
10. Diabetes Genetics Initiative of Broad Institute of Harvard, MIT, Lund University, Novartis Institutes of BioMedical Research, Saxena R, Voight BF, Lyssenko V, Burtt NP, de Bakker PI, Chen H, Roix JJ, Kathiresan S, Hirschhorn JN, Daly MJ, Hughes TE, Groop L, Altshuler D, Almgren P, Florez JC, Meyer J, Ardlie K, Bengtsson Boström K, Isomaa B, Lettre G, Lindblad U, Lyon HN, Melander O, Newton-Cheh C, Nilsson P, Orho-Melander M, Råstam L, Speliotes EK, Taskinen MR, Tuomi T, Guiducci C, Berglund A, Carlson J, Gianniny L, Hackett R, Hall L, Holmkvist J, Laurila E, Sjögren M, Sterner M, Surti A, Svensson M, Svensson M, Tewhey R, Blumenstiel B, Parkin M, Defelice M, Barry R, Brodeur W, Camarata J, Chia N, Fava M, Gibbons J, Handsaker B, Healy C, Nguyen K, Gates C, Sougnez C, Gage D, Nizzari M, Gabriel SB, Chirn GW, Ma Q, Parikh H, Richardson D, Ricke D, Purcell S 2007 Genome-wide association analysis identifies loci for type 2 diabetes and triglyceride levels. Science 316: 1331–1336
11. Sladek R, Rocheleau G, Rung J, Dina C, Shen L, Serre D, Boutin P, Vincent D, Belisle A, Hadjadj S, Balkau B, Heude B, Charpentier G, Hudson TJ, Montpetit A, Pshezhetsky AV, Prentki M, Posner BI, Balding DJ, Meyre D, Polychronakos C, Froguel P 2007 A genome-wide association study identifies novel risk loci for type 2 diabetes. Nature 445:881–885
12. Steinthorsdottir V, Thorleifsson G, Reynisdottir I, Benediktsson R, Jonsdottir T, Walters GB, Styrkarsdottir U, Gretarsdottir S, Emilsson V, Ghosh S, Baker A, Snorradottir S, Bjarnason H, Ng MC, Hansen T, Bagger Y, Wilensky RL, Reilly MP, Adeyemo A, Chen Y, Zhou J, Gudnason V, Chen G, Huang H, Lashley K, Doumatey A, So WY, Ma RC, Andersen G, Borch-Johnsen K, Jorgensen T, van Vliet-Ostaptchouk JV, Hofker MH, Wijmenga C, Christiansen C, Rader DJ, Rotimi C, Gurney M, Chan JC, Pedersen O, Sigurdsson G, Gulcher JR, Thorsteinsdottir U, Kong A, Stefansson K 2007 A variant in *CDKAL1* influences insulin response and risk of type 2 diabetes. Nat Genet 39:770–775
13. Frayling TM, Timpson NJ, Weedon MN, Zeggini E, Freathy RM, Lindgren CM, Perry JR, Elliott KS, Lango H, Rayner NW, Shields B, Harries LW, Barrett JC, Ellard S, Groves CJ, Knight B, Patch AM, Ness AR, Ebrahim S, Lawlor DA, Ring SM, Ben-Shlomo Y, Jarvelin MR, Sovio U, Bennett AJ, Melzer D, Ferrucci L, Loos RJ, Barroso I, Wareham NJ, Karpe F, Owen KR, Cardon LR, Walker M, Hitman GA, Palmer CN, Doney AS, Morris AD, Smith GD, Hattersley AT, McCarthy MI 2007 A common variant in the FTO gene is associated with body mass index and predisposes to childhood and adult obesity. Science 316:889–894
14. Zeggini E, Weedon MN, Lindgren CM, Frayling TM, Elliott KS, Lango H, Timpson NJ, Perry JR, Rayner NW, Freathy RM, Barrett JC, Shields B, Morris AP, Ellard S, Groves CJ, Harries LW, Marchini JL, Owen KR, Knight B, Cardon LR, Walker M, Hitman GA, Morris AD, Doney AS, Wellcome Trust Case Control Consortium (WTCCC), McCarthy MI, Hattersley AT 2007 Replication of genome-wide association signals in UK samples reveals risk loci for type 2 diabetes. Science [Erratum (2007) 317:1035–1036] 316:1336–1341

15. Horikoshi M, Hara K, Ito C, Shojima N, Nagai R, Ueki K, Froguel P, Kadowaki T 2007 Variations in the *HHEX* gene are associated with increased risk of type 2 diabetes in the Japanese population. Diabetologia 50:2461–2466
16. Pascoe L, Tura A, Patel SK, Ibrahim IM, Ferrannini E, Zeggini E, Weedon MN, Mari A, Hattersley AT, McCarthy MI, Frayling TM, Walker M, RISC Consortium, U.K. Type 2 Diabetes Genetics Consortium 2007 Common variants of the novel type 2 diabetes genes *CDKAL1* and *HHEX/IDE* are associated with decreased pancreatic β-cell function. Diabetes 56:3101–3104
17. Grarup N, Rose CS, Andersson EA, Andersen G, Nielsen AL, Albrechtsen A, Clausen JO, Rasmussen SS, Jørgensen T, Sandbaek A, Lauritzen T, Schmitz O, Hansen T, Pedersen O 2007 Studies of association of variants near the *HHEX, CDKN2A/B*, and *IGF2BP2* genes with type 2 diabetes and impaired insulin release in 10,705 Danish subjects: validation and extension of genome-wide association studies. Diabetes 56:3105–3111
18. Furukawa Y, Shimada T, Furuta H, Matsuno S, Kusuyama A, Doi A, Nishi M, Sasaki H, Sanke T, Nanjo K 2008 Polymorphisms in the *IDE-KIF11-HHEX* gene locus are reproducibly associated with type 2 diabetes in a Japanese population. J Clin Endocrinol Metab 93:310–314
19. Omori S, Tanaka Y, Takahashi A, Hirose H, Kashiwagi A, Kaku K, Kawamori R, Nakamura Y, Maeda S 2008 Association of *CDKAL1, IGF2BP2, CDKN2A/B, HHEX, SLC30A8*, and *KCNJ11* with susceptibility to type 2 diabetes in a Japanese population. Diabetes 57:791–795
20. Florez JC, Jablonski KA, Bayley N, Pollin TI, de Bakker PI, Shuldiner AR, Knowler WC, Nathan DM, Altshuler D, Diabetes Prevention Program Research Group 2006 *TCF7L2* polymorphisms and progression to diabetes in the Diabetes Prevention Program. N Engl J Med 355:241–250

nature genetics

Variants in *KCNQ1* are associated with susceptibility to type 2 diabetes mellitus

Kazuki Yasuda[1], Kazuaki Miyake[2], Yukio Horikawa[3], Kazuo Hara[4], Haruhiko Osawa[5], Hiroto Furuta[6], Yushi Hirota[2], Hiroyuki Mori[2], Anna Jonsson[7], Yoshifumi Sato[8], Kazuya Yamagata[8,27], Yoshinori Hinokio[9], He-Yao Wang[1,27], Toshihito Tanahashi[10], Naoto Nakamura[11], Yoshitomo Oka[9], Naoko Iwasaki[12], Yasuhiko Iwamoto[12], Yuichiro Yamada[13,27], Yutaka Seino[13,27], Hiroshi Maegawa[14], Atsunori Kashiwagi[14], Jun Takeda[3], Eiichi Maeda[15], Hyoung Doo Shin[16], Young Min Cho[17], Kyong Soo Park[17], Hong Kyu Lee[17], Maggie C Y Ng[18], Ronald C W Ma[18], Wing-Yee So[18], Juliana C N Chan[18], Valeriya Lyssenko[7], Tiinamaija Tuomi[19,20], Peter Nilsson[21], Leif Groop[7,19], Naoyuki Kamatani[22], Akihiro Sekine[23,27], Yusuke Nakamura[23], Ken Yamamoto[24], Teruhiko Yoshida[25], Katsushi Tokunaga[26], Mitsuo Itakura[10], Hideichi Makino[5], Kishio Nanjo[6], Takashi Kadowaki[4] & Masato Kasuga[2]

We carried out a multistage genome-wide association study of type 2 diabetes mellitus in Japanese individuals, with a total of 1,612 cases and 1,424 controls and 100,000 SNPs. The most significant association was obtained with SNPs in *KCNQ1*, and dense mapping within the gene revealed that rs2237892 in intron 15 showed the lowest *P* value (6.7×10^{-13}, odds ratio (OR) = 1.49). The association of *KCNQ1* with type 2 diabetes was replicated in populations of Korean, Chinese and European ancestry as well as in two independent Japanese populations, and meta-analysis with a total of 19,930 individuals (9,569 cases and 10,361 controls) yielded a *P* value of 1.7×10^{-42} (OR = 1.40; 95% CI = 1.34–1.47) for rs2237892. Among control subjects, the risk allele of this polymorphism was associated with impairment of insulin secretion according to the homeostasis model assessment of β-cell function or the corrected insulin response. Our data thus implicate *KCNQ1* as a diabetes susceptibility gene in groups of different ancestries.

In Japan, the prevalence of type 2 diabetes mellitus is increasing rapidly, and more than 10% of individuals over 40 years of age are affected. Relatively few diabetic individuals in Japan are obese, and impairment of insulin secretion often develops before the onset of diabetes[1]. As part of a national project designated the Millennium Genome Project in Japan, in 2002 we began a multistage genome-wide association study (GWAS) to identify disease-associated SNPs for type 2 diabetes mellitus using 100,000 SNPs from a collection of

[1]Department of Metabolic Disorder, Research Institute, International Medical Center of Japan, Tokyo 162-8655, Japan. [2]Division of Diabetes, Metabolism, and Endocrinology, Department of Internal Medicine, Kobe University Graduate School of Medicine, Kobe 650-0017, Japan. [3]Department of Diabetes and Endocrinology, Division of Molecule and Structure, Gifu University School of Medicine, Gifu 501-1194, Japan. [4]Department of Metabolic Diseases, Graduate School of Medicine, University of Tokyo, Tokyo 113-8655, Japan. [5]Department of Molecular and Genetic Medicine, Ehime University Graduate School of Medicine, Ehime 791-0295, Japan. [6]First Department of Medicine, Wakayama Medical University, Wakayama 641-8509, Japan. [7]Department of Clinical Sciences, Diabetes and Endocrinology, University Hospital Malmö, Lund University, S-205 02 Malmö, Sweden. [8]Department of Metabolic Medicine, Graduate School of Medicine, Osaka University, Osaka 565-0871, Japan. [9]Division of Molecular Metabolism and Diabetes, Tohoku University Graduate School of Medicine, Sendai 980-8574, Japan. [10]Division of Genetic Information, Institute for Genome Research, University of Tokushima, Tokushima 770-8503, Japan. [11]Department of Endocrinology and Metabolism, Kyoto Prefectural University of Medicine, Graduate School of Medical Sciences, Kyoto 602-8566, Japan. [12]Department of Medicine, Diabetes Center, Tokyo Women's Medical University, Tokyo 162-8666, Japan. [13]Department of Diabetes and Clinical Nutrition, Kyoto University School of Medicine, Kyoto 606-8501, Japan. [14]Division of Endocrinology and Metabolism, Department of Medicine, Shiga University of Medical Science, Shiga 520-2192, Japan. [15]Clinical Genome Informatics Center, Kobe University Graduate School of Medicine, Kobe 650-0017, Japan. [16]Department of Genetic Epidemiology, SNP Genetics Inc., Seoul 110-834, Korea. [17]Department of Internal Medicine, Seoul National University College of Medicine, Seoul 110-744, Korea. [18]Department of Medicine and Therapeutics, The Chinese University of Hong Kong, Shatin, Hong Kong. [19]Department of Medicine, Helsinki University Hospital, FIN-00300 Helsinki, Finland. [20]Folkhaelsan Research Center, FIN-00014 Helsinki, Finland. [21]Department of Clinical Sciences, Medicine Research Unit, University Hospital Malmö, Lund University, S-205 02 Malmö, Sweden. [22]Division of Genomic Medicine, Department of Advanced Biomedical Engineering and Science, Tokyo Women's Medical University, Tokyo 162-8666, Japan. [23]SNP Research Center, Institute of Physical and Chemical Research (RIKEN), Yokohama 230-0045, Japan. [24]Department of Molecular Genetics, Medical Institute of Bioregulation, Kyushu University, Fukuoka 812-8582, Japan. [25]Genetics Division, National Cancer Center Research Institute, Tokyo 104-0045, Japan. [26]Department of Human Genetics, Graduate School of Medicine, University of Tokyo, Tokyo 113-0033, Japan. [27]Present addresses: Department of Medical Biochemistry, Faculty of Medical and Pharmaceutical Sciences, Kumamoto University, Kumamoto 860-8556, Japan (K. Yamagata), Shanghai Institute of Materia Medica, Chinese Academy of Science, Shanghai 200031, China (H.-Y.W.), Department of Internal Medicine, Akita University School of Medicine, Akita 010-8543, Japan (Y.Y.), Kansai Electric Power Hospital, Osaka 553-0003, Japan (Y. Seino) and Genome Informatics, Center for Genomic Medicine, Graduate School of Medicine and Faculty of Medicine, Kyoto University, Kyoto 606-8501, Japan (A.S.). Correspondence should be addressed to M.K. (kasuga@med.kobe-u.ac.jp).

Received 3 March; accepted 6 June; published online 17 August 2008; doi:10.1038/ng.207

Table 1 Positive SNPs identified in the third screening

				Panel 1 (187 cases)				Panel 2 (752 cases, 752 controls)				Panel 3 (672 cases, 672 controls)			
dbSNP ID	Risk allele	Chr.	Gene	RAF(DM)	RAF(NC)	OR (95% CI)	*P* value	Control	RAF(DM)	RAF(NC)	OR (95% CI)	*P* value	RAF(DM)	RAF(NC)	OR (95% CI)	*P* value
rs151290	C	11	*KCNQ1*	0.63	0.57	1.30 (1.03–1.65)	0.027	ODG	0.62	0.55	1.34 (1.16–1.55)	7.4×10^{-5}	0.61	0.54	1.36 (1.16–1.58)	1.1×10^{-4}
rs163184	G	11	*KCNQ1*	0.51	0.43	1.33 (1.06–1.67)	0.015	JDC	0.49	0.44	1.22 (1.06–1.41)	0.0064	0.48	0.42	1.27 (1.09–1.48)	0.0021
rs2237895	C	11	*KCNQ1*	0.45	0.35	1.53 (1.22–1.93)	2.8×10^{-4}	JDC	0.42	0.33	1.49 (1.28–1.73)	1.4×10^{-7}	0.42	0.33	1.45 (1.24–1.70)	3.4×10^{-6}
rs2250402	C	15	*EIF2AK4*	0.20	0.27	1.45 (1.09–1.93)	0.011	JDC	0.24	0.21	1.20 (1.01–1.43)	0.035	0.26	0.21	1.34 (1.11–1.60)	0.0018
rs2307027	C	12	*KRT4*	0.14	0.22	1.68 (1.20–2.36)	0.0024	ODG	0.20	0.17	1.23 (1.02–1.47)	0.031	0.21	0.16	1.37 (1.12–1.67)	0.0017
rs3741872	C	12	*FAM60A*	0.29	0.23	1.37 (1.06–1.76)	0.015	ODG	0.29	0.24	1.29 (1.09–1.52)	0.0024	0.28	0.23	1.28 (1.07–1.52)	0.0060
rs574628	G	20	*ANGPT4*	0.56	0.64	1.38 (1.09–1.74)	0.0066	ODG	0.65	0.61	1.17 (1.01–1.36)	0.037	0.64	0.59	1.28 (1.10–1.50)	0.0018
rs2233647	G	6	*SPDEF*	0.92	0.86	1.87 (1.07–3.27)	0.026	ODG	0.88	0.86	1.24 (1.00–1.54)	0.047	0.89	0.86	1.29 (1.02–1.62)	0.033
rs3785233[a]	C	16	*A2BP1*	0.20	0.17	1.20 (0.90–1.61)	0.22	ODG	0.19	0.16	1.25 (1.03–1.51)	0.023	0.19	0.16	1.23 (1.01–1.50)	0.039
rs2075931	A	1		0.71	0.64	1.37 (1.07–1.75)	0.013	ODG	0.68	0.65	1.17 (1.01–1.37)	0.038	0.68	0.64	1.18 (1.00–1.38)	0.048

P values were calculated for allele data. For panel 1, two control groups (ODG, other disease group; JDC, Japanese database control) were used for association studies and the lower *P* values are listed. RAF(DM) and RAF(NC), risk allele frequencies in cases and controls, respectively. OR, odds ratio for risk allele.
[a]This SNP was selected for the second stage on the basis of the recessive model (OR = 2.59, CI = 1.20–5.58, $P = 0.012$).

standard Japanese SNPs[2] (which we refer to as the JSNP Genome Scan (JGS)), as part of the multi-disease collaborative genome scan (**Supplementary Fig. 1** online).

Among 100,000 SNPs genotyped by multiplex PCR–based Invader analysis in the first stage of the study, 82,343 autosomal polymorphisms passed our typing quality control in 187 individuals with diabetes (**Supplementary Table 1** online). We then carried out two separate association analyses to compare the 187 individuals with diabetes with two different control groups, which we considered as population controls: one to compare allele frequencies with reference data for 752 individuals representing the general Japanese population deposited in the JSNP database (referred to as the 'JSNP database control' (JDC)), and one to compare allele or genotype frequencies with those of the 752 individuals in the initial panels for the other four disease groups (Alzheimer's disease, gastric cancer, hypertension and asthma) of the national project (referred to as the 'other disease group' (ODG)). The combination of two types of association analysis resulted in the selection of 2,880 SNPs for the second stage of the study. An independent case-control panel (panel 2) was analyzed, and 201 positive SNPs ($P < 0.05$) were selected for the third stage (see **Supplementary Table 2a** online). Ten SNPs yielded a *P* value of <0.05 at the third stage using another case-control panel (panel 3; **Table 1** and **Supplementary Table 2b**). These SNPs showed variable *P* values in the first stage, suggestive of a limited power of the study design. The most significant association ($P = 3.4 \times 10^{-6}$) was obtained with rs2237895, which is located in intron 15 of *KCNQ1*. Another two SNPs (rs151290 and rs163184) were also located in the same intron, yielding *P* values of 1.1×10^{-4} and 0.0021, respectively. Panels 2 and 3 combined (panel 2+3) were analyzed for these 10 SNPs, yielding even lower *P* values for all the SNPs (**Supplementary Table 2b**). The genotype-based Cochran-Armitage trend test gave *P* values similar to those based on the allele data (**Supplementary Table 2b**).

We further analyzed *KCNQ1*, which was the only gene that yielded positive results according to the standard criterion (*P* value of $<5 \times 10^{-7}$) recently proposed for GWAS[3]. The three SNPs of *KCNQ1* that passed the third scan (rs151290, rs163184 and rs2237895) were in moderate linkage disequilibrium (LD) with each other (**Fig. 1**). The SNP with the lowest *P* value, rs2237895, yielded D' and r^2 values of 0.54 and 0.12 with rs151290 and 0.83 and 0.46 with rs163184, respectively. We isolated 49 additional SNPs of *KCNQ1* from dbSNP of NCBI and typed them together with the three originally positive SNPs in panel 2+3 (**Fig. 1**). Among these 52 SNPs, rs2237892, which is also located in intron 15, showed the strongest association with diabetes ($P = 6.7 \times 10^{-13}$), with OR =1.49 and 95% CI = 1.34–1.66; the *P* value for the trend test was 1.7×10^{-12} (**Table 2**). The D' and r^2 values for rs2237895 and rs2237892 were 0.95 and 0.30, respectively.

We also sequenced all the exons and the 47-kb genomic region corresponding to intron 15 of *KCNQ1* in 24 Japanese individuals and identified 212 variations, including three synonymous and two nonsynonymous (P448R and G643S) polymorphisms (**Supplementary Table 3a** online). We then genotyped ten of the newly identified SNPs of intron 15 and the two nonsynonymous polymorphisms in panel 2+3. None of these SNPs showed a stronger association with diabetes than did rs2237892 (**Fig. 1** and **Supplementary Table 3b**).

We next examined the possible association of *KCNQ1* with diabetes in several additional subject panels, including those of other ancestral groups, by genotyping rs2237892, rs2237895 and rs2074196, the three SNPs that showed the strongest association in the original study. Two independent Japanese panels revealed a strong association of these

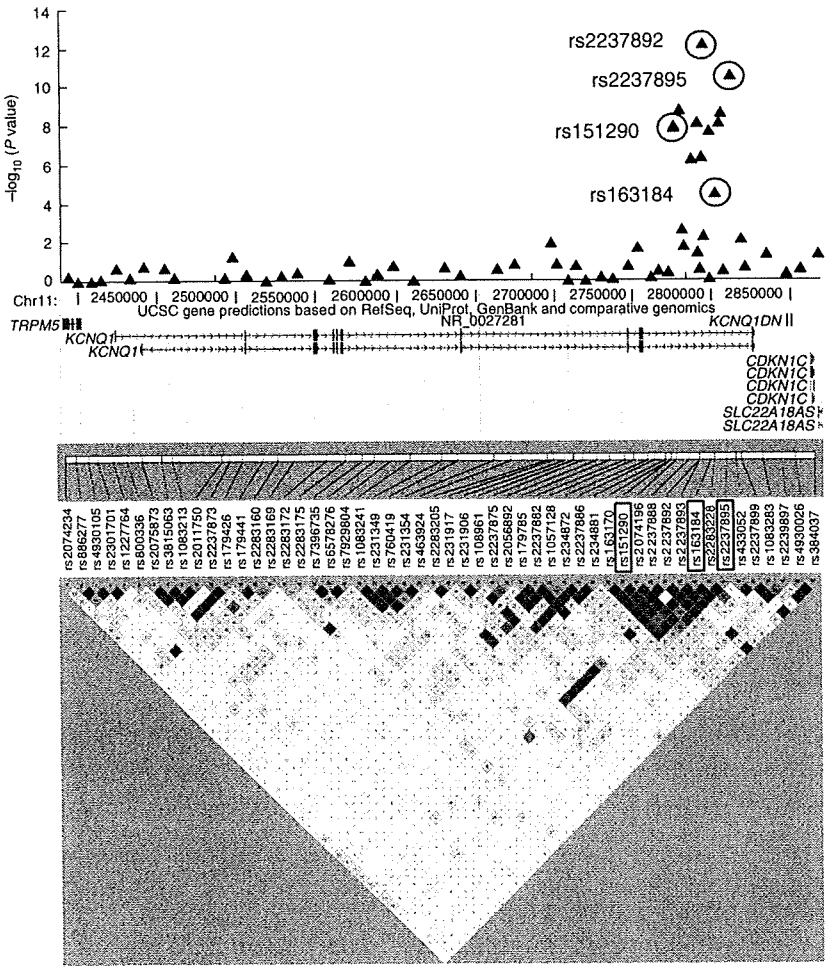

Figure 1 Dense mapping analysis of *KCNQ1*. The top panel shows the association $-\log_{10}$ (*P* value) in panel 2+3 for 64 SNPs of *KCNQ1*. The three blue circles represent the positive SNPs in the third screening. The red circle (rs2237892) indicates the SNP showing the most significant association with type 2 diabetes. The upper middle panel shows the physical position of *KCNQ1* and neighboring genes on chromosome 11 (UCSC Genome Browser). The lower middle panel shows the positions and rs numbers of the 52 previously identified SNPs. Blue rectangles indicate the positive SNPs in the third screening. The bottom panel shows a Haploview representation of LD (*D'*) based on genotyping data from control subjects in panel 2+3 (n = 1,424).

polymorphisms with diabetes (**Table 2** and **Supplementary Table 4** online); rs2237892, for example, showed allelic *P* values of 9.6×10^{-10} and 6.9×10^{-10} in the replication 1 and 2 panels, respectively. The three Japanese panels (panel 2+3 and replication 1 and 2), which included a total of 4,378 cases and 4,412 controls, yielded an allelic *P* value of 2.8×10^{-29} and OR of 1.43 (95% CI = 1.34–1.52) for rs2237892. The association was also reproduced in the replication 3 (Chinese) and replication 4 (Korean) panels; the allelic *P* values for rs2237892 in these two panels were 1.3×10^{-8} and 1.7×10^{-5}, respectively (**Table 2** and **Supplementary Table 4**). Meta-analysis of the Asian populations yielded a *P* value of 2.5×10^{-40} and OR of 1.42 (95% CI = 1.34–1.49) for rs2237892. We also examined rs2237892 and rs2074196 in the replication 5 panel (recruited from Sweden), with both SNPs showing a positive association ($P = 7.8 \times 10^{-4}$ and 0.017, respectively). With the inclusion of the replication 5 panel, meta-analysis with a total of 19,930 individuals (9,569 cases and 10,361 controls) yielded a *P* value of 1.7×10^{-42} and OR of 1.40 (95% CI = 1.34–1.47) for rs2237892 (**Table 2** and **Supplementary Fig. 2** online).

We next investigated the relation of rs2237892 to clinical phenotype. Among 1,424 individuals with diabetes in panel 2+3, no association was found between this SNP and clinical parameters such as body mass index (BMI) and the level of insulin resistance. Among the 948 control subjects in panel 2+3 whose fasting plasma glucose and insulin levels were available, homozygotes for the risk allele of rs2237892 (CC) showed a significantly lower homeostasis model assessment of β-cell function (HOMA-β)[4] than did those with the other genotypes (**Supplementary Table 5** online). Among nondiabetic subjects of the Botnia prospective cohort (**Supplementary Methods** online), the corrected insulin response (CIR) at the follow-up visit was significantly lower for individuals with the CC genotype of rs2237892 than for those with the other two genotypes in both an additive and recessive model for this SNP (P = 0.024 and 0.010, respectively; **Supplementary Table 5**). These results suggested that the risk allele of *KCNQ1* might contribute to diabetes susceptibility by impairing insulin secretion.

The multistage strategy for GWASs has an advantage in the effective elimination of a large number of false-positive results and has proved to be successful[5]. Indeed, we detected the association of several SNPs of *KCNQ1* with diabetes in the JGS, and this association was reproduced in two independent Japanese panels. *KCNQ1*, which encompasses 404 kb, is located at chromosome 11p15.5, not far from a candidate region at 11p13–p12 with suggestive evidence of linkage to type 2 diabetes in two independent studies of affected Japanese sibpairs[6,7]. We also reproduced the association of *KCNQ1* with diabetes in Chinese and Korean panels, establishing *KCNQ1* as a diabetes susceptibility gene for populations of East Asian descent. We further showed the association to be significant in individuals of European descent. Given that *KCNQ1* was not implicated as a diabetes susceptibility gene in two recent GWASs with individuals of European descent[8,9], we examined SNPs of *KCNQ1* in the available datasets (**Supplementary Fig. 3** and **Supplementary Table 6a,b** online). Within the LD block of *KCNQ1* that includes the SNPs associated with diabetes in Japanese, 11 SNPs in the WTCCC dataset[8] and 9 SNPs in the DGI dataset[9] had been typed, and none of them had been selected for further analysis. This apparent discrepancy may be due mainly to the allele frequencies of the causative SNPs (the minor allele frequency of rs2237892 was 0.28–0.41 and 0.05–0.07 in populations of East Asian and European descent, respectively). Indeed, in a recent meta-analysis of three GWASs (DGI, WTCCC and FUSION; see URLs section in Methods)[10], the risk alleles of both rs2237892 and rs2074196 identified in the present study were associated with an increased risk of type 2 diabetes (P = 0.01 and 0.02,

Table 2 Association study results for SNPs in *KCNQ1* and type 2 diabetes

SNP ID	Risk allele	Panel	RAF(DM)	RAF(NC)	P_{allele}	OR	95% CI		P_{trend}	Meta-analysis OR (95% CI) *P* value
rs2074196	G	2+3 (dense mapping)	0.63	0.55	1.7×10^{-9}	1.39	1.25	1.54	1.8×10^{-9}	
		Replication 1 (Japanese)	0.61	0.54	1.4×10^{-7}	1.32	1.19	1.46	2.1×10^{-7}	
		Replication 2 (Japanese)	0.62	0.55	4.7×10^{-7}	1.31	1.18	1.46	6.2×10^{-7}	
		All Japanese (4,378 cases, 4,412 controls)	**0.62**	**0.55**	**4.6×10^{-21}**	**1.34**	**1.26**	**1.42**	**9.8×10^{-21}**	**1.34 (1.26–1.42), $P = 4.8 \times 10^{-21}$**
		Replication 3 (Chinese)	0.71	0.63	1.2×10^{-9}	1.40	1.26	1.56	9.8×10^{-10}	
		Replication 4 (Korean)	0.66	0.58	3.0×10^{-5}	1.39	1.19	1.62	2.1×10^{-5}	
		All Asian (6,552 cases, 6,621 controls)	**0.64**	**0.57**	**9.9×10^{-32}**	**1.35**	**1.28**	**1.42**	**2.1×10^{-31}**	**1.36 (1.29–1.42), $P = 7.9 \times 10^{-33}$**
		Replication 5 (European)	0.96	0.95	0.017	1.23	1.04	1.46	0.017	
		All	n.a.	n.a.	n.a.	n.a.	n.a.	n.a.	n.a.	**1.35 (1.28–1.41), $P = 8.6 \times 10^{-34}$**
rs2237892	C	2+3 (dense mapping)	0.69	0.60	6.7×10^{-13}	1.49	1.34	1.66	1.7×10^{-12}	
		Replication 1 (Japanese)	0.66	0.59	9.6×10^{-10}	1.39	1.25	1.54	1.6×10^{-9}	
		Replication 2 (Japanese)	0.68	0.60	6.9×10^{-10}	1.41	1.26	1.57	1.1×10^{-9}	
		All Japanese (4,378 cases, 4,412 controls)	**0.68**	**0.59**	**2.8×10^{-29}**	**1.43**	**1.34**	**1.52**	**1.7×10^{-28}**	**1.43 (1.34–1.52), $P = 3.0 \times 10^{-29}$**
		Replication 3 (Chinese)	0.72	0.65	1.3×10^{-8}	1.38	1.24	1.55	4.2×10^{-9}	
		Replication 4 (Korean)	0.69	0.61	1.7×10^{-5}	1.41	1.21	1.65	1.0×10^{-5}	
		All Asian (6,552 cases, 6,621 controls)	**0.69**	**0.61**	**2.0×10^{-39}**	**1.41**	**1.34**	**1.48**	**2.5×10^{-39}**	**1.42 (1.34–1.49), $P = 2.5 \times 10^{-40}$**
		Replication 5 (European)	0.95	0.93	7.8×10^{-4}	1.29	1.11	1.50	7.2×10^{-4}	
		All	n.a.	n.a.	n.a.	n.a.	n.a.	n.a.	n.a.	**1.40 (1.34–1.47), $P = 1.7 \times 10^{-42}$**
rs2237895	C	2+3 (dense mapping)	0.41	0.33	3.1×10^{-11}	1.44	1.30	1.61	4.0×10^{-11}	
		Replication 1 (Japanese)	0.38	0.33	4.5×10^{-5}	1.25	1.12	1.38	4.7×10^{-5}	
		Replication 2 (Japanese)	0.41	0.34	5.8×10^{-8}	1.35	1.21	1.50	5.5×10^{-8}	
		All Japanese (4,378 cases, 4,412 controls)	**0.40**	**0.33**	**1.3×10^{-20}**	**1.34**	**1.26**	**1.43**	**1.7×10^{-20}**	**1.34 (1.26–1.43), $P = 1.4 \times 10^{-20}$**
		Replication 3 (Chinese)	0.40	0.34	3.5×10^{-5}	1.25	1.12	1.39	3.4×10^{-5}	
		Replication 4 (Korean)	0.35	0.30	3.2×10^{-3}	1.27	1.08	1.49	2.7×10^{-3}	
		All Asian (6,552 cases, 6,621 controls)	**0.39**	**0.33**	**2.7×10^{-25}**	**1.31**	**1.24**	**1.38**	**2.7×10^{-25}**	**1.31 (1.25–1.38), $P = 6.1 \times 10^{-26}$**
		Replication 5 (European)	n.a.	n.a.	n.a.	n.a.	n.a.	n.a.	n.a.	

RAF(DM) and RAF(NC), risk allele frequencies in cases and controls, respectively. P_{allele} values were calculated for allele data. OR, odds ratio for risk allele. P_{trend} values were calculated by the Cochran-Armitage trend test. Meta-analysis was performed by the Mantel-Haenszel method (fixed-effects models). n.a., not applicable.

respectively). These results provide further support for *KCNQ1* as a general susceptibility gene for diabetes, and they also highlight the need to extend GWAS to different populations.

Alternative splicing has been found to generate several variants of *KCNQ1* mRNA (see Accession codes section in Methods), but we do not know whether the identified candidate SNPs in intron 15 affect the splicing pattern of the primary transcript. Although neighboring genes seem to be located outside the LD block containing rs2237892, we are not able to exclude completely the possibility that the SNPs identified in the present study affect the expression of other causative genes. We did not find any microRNA harboring rs2237892 in the miRBase database.

KCNQ1 encodes the pore-forming subunit of a voltage-gated K^+ channel (KvLQT1) that is essential for the repolarization phase of the action potential in cardiac muscle[11]. Mutations in this gene are associated with cardiac diseases such as hereditary long QT syndrome (Romano-Ward syndrome[12] and Jervell and Lange-Nielsen syndrome[13]) and familial atrial fibrillation[14]. This K^+ channel is also expressed in other tissues, including brain, adipose tissues and pancreas[15,16]. The lower HOMA-β or CIR apparent for CC homozygotes of rs2237892 among Japanese and Europeans in the present study may reflect a functional role for this channel in insulin-producing cells. We examined the abundance of *Kcnq1* mRNA by reverse transcription and real-time PCR analysis in the islets of 12-week-old diabetic KK-Ay mice, which manifested both hyperglycemia and hyperinsulinemia. The amount of the mRNA was significantly increased ($P = 0.0004$) by a factor of 1.6 compared with that in the islets of C57BL6 control mice (data not shown). The KCNQ1 protein was previously shown to be expressed in insulin-secreting INS-1 cells, and the KCNQ1 blocker 293B was found to stimulate insulin secretion in the presence of tolbutamide[17]. It is also possible that fine-tuning of the membrane potential by this channel might modulate the survival of pancreatic β cells in the long term. Further studies are necessary to elucidate the precise mechanism by which the risk allele of *KCNQ1* confers susceptibility to diabetes.

We may have missed a substantial number of susceptibility genes in our screening, given that the strategy we adopted seven years ago lacks sufficient analytical power[18] relative to that now achievable as a result of recent progress in genomic studies. The genomic coverage of the SNP set was not robust, in part because the IMS-JST Japanese SNP (JSNP) database was designed to focus on 'gene-centric' SNPs[2]. Several comprehensive studies based on new platforms for GWASs have recently been described, with about ten genes being found to be

reproducibly associated with type 2 diabetes in individuals of European ancestry[8,9,19–23]. None of these genes showed a positive association in our JGS typing data. Given that some of these genes were recently shown to confer susceptibility to diabetes in Japanese[24–26], the lack of association in our study might be due to the limited sample size of the first scan or to weak LD between the SNPs we used and the causative variants; actually, some genes were totally missed in our JGS (**Supplementary Table 6c**).

In summary, with a comprehensive multistage SNP association study in Japanese, we have identified *KCNQ1* as a previously unreported susceptibility gene as well as several other candidate genes for type 2 diabetes mellitus. Replication studies further confirmed the association of *KCNQ1* with diabetes in individuals of East Asian and European descent. Our findings may provide new insight into the pathophysiology of diabetes as well as a basis for the development of new therapeutic agents.

METHODS

Study participants. We assembled three independent subject panels for multistage genome-wide screening. Panel 1 consisted of 188 cases only, panel 2 of 752 cases and 752 controls and panel 3 of 672 cases and 672 controls. The inclusion criteria for diabetic patients were as follows: (i) age of disease onset of 40 to 55 years, (ii) maximum BMI of <30 kg/m^2, (iii) insulin treatment not initiated until at least three years after diagnosis and (iv) absence of antibodies to glutamic acid decarboxylase. Most Japanese diabetic individuals have a BMI of <30 kg/m^2, and we aimed to focus on the most common subtype of type 2 diabetes in Japan. The criteria for controls in panels 2 and 3 were as follows: (i) age of >60 years, (ii) no past history of diagnosis of diabetes and (iii) hemoglobin A_{1c} content of $<5.6\%$. The cases in the three panels and the controls in panels 2 and 3 were recruited at 11 core facilities located in various regions of Japan. Panels 2 and 3 were assembled simultaneously. Genomic DNA was extracted from peripheral blood by standard methods. We also obtained clinical information such as BMI, blood biochemistry (including plasma glucose and insulin levels) and family history of diabetes. The replication panels are described in **Supplementary Methods**. The clinical characteristics of subjects in each panel are summarized in **Supplementary Table 1**. The study protocol was approved by the local ethics committee of each institution, and written informed consent was obtained from all participants.

Study design. The general design and power for the multistage screening in the Millennium Genome Project (**Supplementary Fig. 1**), referred to as the JSNP Genome Scan (JGS), have been described previously[18]. In the first stage, 188 individuals with each disease (panel 1 for diabetes) were genotyped for 100,000 SNPs in the IMS-JST JSNP database (see URLs section below)[2]. The coverage of the nucleotide sequences of the RefSeq NM exonic regions (as defined by 5′ UTR + CDS (coding sequences) + 3′ UTR) achieved by the JSNP 'gene-centric' genome-wide LD mapping is estimated to be $\sim 35\%$, if we assume an average extent of LD of 10 kb for each SNP with a minor allele frequency (MAF) of $>15\%$. We also previously evaluated the power of the first two stages of the JGS by a simulation experiment[18]. For example, this analysis would yield a sensitivity of $\sim 13\%$ for SNPs with an odds ratio of 1.5 and a disease-associated genotype frequency of 30%.

One subject did not yield a genotype call for any SNP in the first stage. We then carried out two separate association analyses to compare the 187 diabetic individuals with two different control groups, which we referred to as JDC and ODG, respectively. We did not detect significant population stratification among individuals of the initial panels of the five disease groups by standard methods such as genomic control[27] (inflation factor = 1.06 with 1,025 SNPs selected for genomic control analysis). The genotype-based analysis was done with dominant and recessive models. First, SNPs whose MAF was $>10\%$ in the database and which showed either a genotype OR of >1.5 or an allele OR of >1.3 in either association analysis were selected. If multiple SNPs in the same gene with positive association were in strong LD ($r^2 > 0.9$), only one SNP was chosen for the next step to avoid redundancy. A total of 2,880 SNPs for each disease was then selected for the second screening in order of P value; for diabetes, 2,343 and 1,111 SNPs were selected by the association analyses with ODG and JDC, respectively, with 574 SNPs being selected by both analyses.

In the second stage, an independent case-control panel (panel 2) was analyzed, generating valid data for 2,827 SNPs after a quality check. Thirty-eight SNPs gave no results for all the samples in panel 2, whereas five and three SNPs yielded no data for all case or control samples, respectively, by multiplex PCR-based Invader analysis, and seven probes were not annotated on the updated human genome. The call rate for the 2,827 SNPs was 0.993. A total of 201 positive SNPs ($P < 0.05$) was selected for the third stage of the study on the basis of allelic data (**Supplementary Table 2a**). In the third stage, another case-control panel (panel 3) was typed; one SNP could not be typed by SSP-PCR-FCS analysis (see below) for any of the subjects in panel 3, with the call rate for the other 200 SNPs being 0.990. The ten positive SNPs ($P < 0.05$; **Table 1**) were also then analyzed in the combined panels 2 and 3 (panel 2+3, 1,424 cases and 1,424 controls). Panel 2 was genotyped again for these ten SNPs by SSP-PCR-FCS analysis, and the concordance rate with the Invader method used in the second screening was 0.992. The possibility of stratification in panels 2 and 3 was assessed by typing of 28 diabetes-unrelated SNPs followed by (i) comparison of allele and genotype frequencies by the χ^2 test, (ii) principal component analysis or (iii) STRUCTURE analysis (see URLs section below). None of these analyses showed evidence of stratification among cases and controls of panels 2 and 3 (data not shown).

The list of SNPs used for the initial screening and the allele and genotype frequency data for the first and the second stages of the JGS for the five diseases studied in the Millennium Genome Project of Japan, including diabetes, have been deposited in the Genome Medicine Database of Japan (GeMDBJ, see URLs section below).

Dense SNP mapping for *KCNQ1*. We first selected 49 additional SNPs of *KCNQ1* from the dbSNP database of NCBI, with an average interval of ~ 10 kbp, and typed these polymorphisms in panel 2+3 together with the three positive SNPs originally included in the JGS. We sequenced 24 control Japanese subjects for the gene, including all the exons and the putative promoter region (4 kbp upstream from the transcription start site), in order to comprehensively identify genetic variants in Japanese. We also sequenced the regions surrounding the positive SNPs of *KCNQ1*, spanning 47 kbp (intron 15). Ten of the SNPs identified in the 47-kbp region were selected on the basis of LD and MAF ($>10\%$). These 10 SNPs and the two identified nonsynonymous variants were genotyped in panel 2+3. A total of 64 SNPs was thus genotyped for *KCNQ1*, including 18 SNPs in the 35.6-kbp region between rs151290 and rs2237895, with an average interval of 2 kbp (see **Supplementary Table 3b**).

Typing methods. In the first and second stages of the study, genotyping was done by the multiplex PCR-based Invader assay (Third Wave Technologies) as previously described[28]. In the third stage and for dense mapping, genome-wide amplified DOP degenerate oligonucleotide–primed (DOP)-PCR templates were genotyped by sequence-specific primer (SSP)-PCR analysis followed by fluorescence correlation spectroscopy (FCS)[29]. Some SNPs included in dense mapping were therefore re-genotyped in panel 2 by the SSP-PCR-FCS method. Some SNPs were genotyped by real-time PCR analysis with TaqMan probes (Applied Biosystems). For replication panels, we applied either SSP-PCR-FCS or the TaqMan method.

Statistical analysis. In the first screening, we performed two case-control evaluations as described above. We examined allele or genotype (dominant or recessive models) data in 2×2 contingency tables for comparison with ODG, as well as allele data in 2×2 contingency tables for comparison with JDC (for which genotype data were not available). In the second and third screening and dense mapping, we analyzed allele data in 2×2 contingency tables by the χ^2 test. LD and haplotype analyses were done with Haploview 3.31 software[30]. A P value of <0.05 was considered statistically significant. For ten positive SNPs in the JGS, rs2237892 and rs2074196, genotype-based analyses were also performed by the Cochran-Armitage trend test. Meta-analysis was done by the Mantel-Haenszel method (fixed-effects models) with the "meta" package of the R Project; the P values for heterogeneity among panels joined in the Mantel-Haenszel tests were all >0.05.

URLs. Genome Medicine Database of Japan, https://gemdbj.nibio.go.jp/dgdb/; DGI, WTCCC and FUSION, http://www.well.ox.ac.uk/DIAGRAM/; miRBase database, http://microrna.sanger.ac.uk/sequences/; IMS-JST JSNP database, http://snp.ims.u-tokyo.ac.jp/; STRUCTURE analysis, http://pritch.bsd.uchicago.edu/software.html.

Accession codes. GenBank: *KCNQ1* mRNA, NM_000218.2 and NM_181798.1.

Note: Supplementary information is available on the Nature Genetics website.

ACKNOWLEDGMENTS

We thank all the participants in the project; S. Sugano and S. Tsuji for support and helpful discussion throughout the project; H. Sakamoto, K. Yoshimura and N. Nishida for genotyping and quality control of the data; M. Yamaoka-Sageshima, K. Nagase, D. Suzuki and A. Berglund for technical assistance; and staff of Mitsui Knowledge Industry Inc. (Tokyo) for help with bioinformatics. This work was supported by a grant from the Program for Promotion of Fundamental Studies in Health Sciences of the Pharmaceuticals and Medical Devices Agency (PMDA) of Japan; a grant from the National Institute of Biomedical Innovation (NIBIO) of Japan; grants from the Ministry of Health, Labour, and Welfare of Japan; a Grant-in-Aid for Scientific Research on Priority Areas (C), "Medical Genome Science (Millennium Genome Project)," "Applied Genomics" and "Comprehensive Genomics" from the Ministry of Education, Culture, Sports, Science, and Technology of Japan; and a grant from New Energy and Industrial Technology Development Organization (NEDO). The replication 2 study was supported by a grant from Cooperative Link of Unique Science and Technology for Economy Revitalization (CLUSTER, Tokushima, Japan). The Hong Kong diabetes case-control study was supported by the Hong Kong Research Grants Committee Central Allocation Scheme CUHK 1/04C. The Korean case-control study was supported by a grant from the Korea Health 21 R&D Project of the Ministry of Health and Welfare of the Republic of Korea (00-PJ3-PG6-GN07-001 to K.S.P.). The replication 5 study and Botnia prospective study were supported by Swedish Research Council (Linne grant), Sigrid Juselius Foundation, Folkhaelsan Research Foundation, European Foundation for the Study of Diabetes and Swedish Diabetes Research Foundation.

AUTHOR CONTRIBUTIONS

Principal investigators: K. Yasuda and M.K. Manuscript writing: K. Yasuda., K.M., Y. Horikawa and M.K. Diabetes project planning and design: K. Yasuda, K.M., Y. Hirota, H. Mori, T.Y. and M.K. Ascertainment of study subjects and general data analyses in Japan: K. Yasuda, K.M., Y. Horikawa, K.H., H.O., H.F., Y. Hirota, H. Mori, Y. Sato, K. Yamagata, Y. Hinokio, H.-Y.W., T. Tanahashi, N.N., Y.O., N.I., Y.I., Y.Y., Y. Seino, H. Maegawa, A.K., J.T., E.M., N.K., M.I., H. Makino, K.N., T.K. and M.K. Genotyping and sequencing analyses in Japan: K.M., Y. Horikawa, Y. Hirota, T. Tanahashi, A.S., Y.N., K. Yamamoto, T.Y., K.T. and M.I. Statistical analyses: K.M., Y. Horikawa, Y. Hirota, E.M., T.Y., K.T. and M.I. Genetic analyses in Korea: H.D.S., Y.M.C., K.S.P. and H.K.L. Genetic analyses in Hong Kong: M.C.Y.N., R.C.W.M., W.-Y.S. and J.C.N.C. Genetic analyses in Europe: A.J., V.L., T. Tuomi, P.N. and L.G. Millennium Genome Project Human Genome Variation Team Leader: Y.N. Millennium Genome Project Diabetes Subteam Leader: M.K.

Published online at http://www.nature.com/naturegenetics/
Reprints and permissions information is available online at http://npg.nature.com/reprintsandpermissions/

1. Fukushima, M., Suzuki, H. & Seino, Y. Insulin secretion capacity in the development from normal glucose tolerance to type 2 diabetes. *Diabetes Res. Clin. Pract.* **66**, S37–S43 (2004).
2. Haga, H., Yamada, R., Ohnishi, Y., Nakamura, Y. & Tanaka, T. Gene-based SNP discovery as part of the Japanese Millennium Genome Project: identification of 190,562 genetic variations in the human genome. *J. Hum. Genet.* **47**, 605–610 (2002).
3. NCI-NHGRI Working Group on Replication in Association Studies. Replicating genotype-phenotype associations. *Nature* **447**, 655–660 (2007).
4. Matthews, D.R. *et al.* Homeostasis model assessment: insulin resistance and beta-cell function from fasting plasma glucose and insulin concentrations in man. *Diabetologia* **28**, 412–419 (1985).
5. Ozaki, K. *et al.* Functional SNPs in the lymphotoxin-alpha gene that are associated with susceptibility to myocardial infarction. *Nat. Genet.* **32**, 650–654 (2002).
6. Mori, Y. *et al.* Genome-wide search for type 2 diabetes in Japanese affected sib-pairs confirms susceptibility genes on 3q, 15q, and 20q and identifies two new candidate loci on 7p and 11p. *Diabetes* **51**, 1247–1255 (2002).
7. Nawata, H. *et al.* Genome-wide linkage analysis of type 2 diabetes mellitus reconfirms the susceptibility locus on 11p13-p12 in Japanese. *J. Hum. Genet.* **49**, 629–634 (2004).
8. Zeggini, E. *et al.* Replication of genome-wide association signals in U.K. samples reveals risk loci for type 2 diabetes. *Science* **316**, 1336–1340 (2007).
9. Saxena, R. *et al.* Genome-wide association analysis identifies loci for type 2 diabetes and triglyceride levels. *Science* **316**, 1331–1336 (2007).
10. Zeggini, E. *et al.* Meta-analysis of genome-wide association data and large-scale replication identifies additional susceptibility loci for type 2 diabetes. *Nat. Genet.* **40**, 638–645 (2008).
11. Barhanin, J. *et al.* K(v)LQT1 and IsK (minK) proteins associate to form the I(Ks) cardiac potassium current. *Nature* **384**, 78–80 (1996).
12. Wang, Q. *et al.* Positional cloning of a novel potassium channel gene: KVLQT1 mutations cause cardiac arrhythmias. *Nat. Genet.* **12**, 17–23 (1996).
13. Neyroud, N. *et al.* A novel mutation in the potassium channel gene KvLQT1 causes the Jervell and Lange-Nielsen cardioauditory syndrome. *Nat. Genet.* **15**, 186–189 (1997).
14. Chen, Y.H. *et al.* KCNQ1 gain-of-function mutation in familial atrial fibrillation. *Science* **299**, 251–254 (2003).
15. Demolombe, S. *et al.* Differential expression of KvLQT1 and its regulator IsK in mouse epithelia. *Am. J. Physiol. Cell Physiol.* **280**, C359–C372 (2001).
16. Chouabe, C. *et al.* Properties of KvLQT1 K^+ channel mutations in Romano-Ward and Jervell and Lange-Nielsen inherited cardiac arrhythmias. *EMBO J.* **16**, 5472–5479 (1997).
17. Ullrich, S. *et al.* Effects of I_{Ks} channel inhibitors in insulin-secreting INS-1 cells. *Pflugers Arch.* **451**, 428–436 (2005).
18. Sato, Y. *et al.* Designing a multistage, SNP-based, genome screen for common diseases. *J. Hum. Genet.* **49**, 669–676 (2004).
19. Grant, S.F. *et al.* Variant of transcription factor 7-like 2 (TCF7L2) gene confers risk of type 2 diabetes. *Nat. Genet.* **38**, 320–323 (2006).
20. Scott, L.J. *et al.* A genome-wide association study of type 2 diabetes in Finns detects multiple susceptibility variants. *Science* **316**, 1341–1345 (2007).
21. Sladek, R. *et al.* A genome-wide association study identifies novel risk loci for type 2 diabetes. *Nature* **445**, 881–885 (2007).
22. Steinthorsdottir, V. *et al.* A variant in CDKAL1 influences insulin response and risk of type 2 diabetes. *Nat. Genet.* **39**, 770–775 (2007).
23. Frayling, T.M. *et al.* A common variant in the FTO gene is associated with body mass index and predisposes to childhood and adult obesity. *Science* **316**, 889–894 (2007).
24. Miyake, K. *et al.* Association of TCF7L2 polymorphisms with susceptibility to type 2 diabetes in 4,087 Japanese subjects. *J. Hum. Genet.* **53**, 174–180 (2008).
25. Horikoshi, M. *et al.* Variations in the HHEX gene are associated with increased risk of type 2 diabetes in the Japanese population. *Diabetologia* **50**, 2461–2466 (2007).
26. Horikawa, Y. *et al.* Replication of genome-wide association studies of type 2 diabetes susceptibility in Japan. *J. Clin. Endocrinol. Metab.* (in the press).
27. Devlin, B. & Roeder, K. Genomic control for association studies. *Biometrics* **55**, 997–1004 (1999).
28. Ohnishi, Y. *et al.* A high-throughput SNP typing system for genome-wide association studies. *J. Hum. Genet.* **46**, 471–477 (2001).
29. Bannai, M. *et al.* Single-nucleotide-polymorphism genotyping for whole-genome-amplified samples using automated fluorescence correlation spectroscopy. *Anal. Biochem.* **327**, 215–221 (2004).
30. Barrett, J.C., Fry, B., Maller, J. & Daly, M.J. Haploview: analysis and visualization of LD and haplotype maps. *Bioinformatics* **21**, 263–265 (2005).

cellular target is the nascent endothelial network of the neural tube. These, and likely other Wnt family members, act through a canonical Wnt signaling pathway to promote formation and differentiation of the CNS vasculature. Whether this pathway also plays a later role in vascularization of other organ systems remains to be determined.

Our findings may have important clinical ramifications. For example, local reductions in Wnt signaling levels could potentially lead to malformation of CNS vasculature. In addition, if BBB properties in the adult are regulated by Wnt, altering Wnt activity may be a fruitful strategy for delivery of pharmacological agents to the CNS. Interestingly, there is a correlation between neoangiogenesis and β*Cat* accumulation in the endothelium of brain tumors such as gliomas and human glioblastoma multiforme (*28*, *29*). This raises the possibility that canonical Wnt signaling may not only support vascular development but also promote tumor pathogenesis in the CNS.

References and Notes

1. A. M. Suburo, P. A. D'Amore, *Handb. Exp. Pharmacol.* **176**, 71 (2006).
2. B. Engelhardt, *Cell Tissue Res.* **314**, 119 (2003).
3. A. M. Miniño, M. P. Heron, B. L. Smith, *Deaths: Preliminary Data for 2004* (National Center for Health Statistics, Hyattsville, MD, 2006).
4. B. A. Parr, M. J. Shea, G. Vassileva, A. P. McMahon, *Development* **119**, 247 (1993).
5. B. A. Parr, A. P. McMahon, *Nature* **395**, 707 (1998).
6. B. A. Parr, V. A. Cornish, M. I. Cybulsky, A. P. McMahon, *Dev. Biol.* **237**, 324 (2001).
7. See supporting material on *Science* Online. The conditional Wnt7b allele is referred to as "c3" and the recombined allele as "d3."
8. K. A. Hogan, C. A. Ambler, D. L. Chapman, V. L. Bautch, *Development* **131**, 1503 (2004).
9. F. Tronche *et al.*, *Nat. Genet.* **23**, 99 (1999).
10. D. Graus-Porta *et al.*, *Neuron* **31**, 367 (2001).
11. M. Backman *et al.*, *Dev. Biol.* **279**, 155 (2005).
12. S. Maretto *et al.*, *Proc. Natl. Acad. Sci. U.S.A.* **100**, 3299 (2003).
13. L. A. Brown *et al.*, *Mech. Dev.* **90**, 237 (2000).
14. T. Motoike, D. W. Markham, J. Rossant, T. N. Sato, *Genesis* **35**, 153 (2003).
15. V. Brault *et al.*, *Development* **128**, 1253 (2001).
16. A. Cattelino *et al.*, *J. Cell Biol.* **162**, 1111 (2003).
17. H. Haegel *et al.*, *Development* **121**, 3529 (1995).
18. J. Huelsken *et al.*, *J. Cell Biol.* **148**, 567 (2000).
19. I. B. Lobov *et al.*, *Nature* **437**, 417 (2005).
20. W. Shu, Y. Q. Jiang, M. M. Lu, E. E. Morrisey, *Development* **129**, 4831 (2002).
21. S. J. Monkley, S. J. Delaney, D. J. Pennisi, J. H. Christiansen, B. J. Wainwright, *Development* **122**, 3343 (1996).
22. T. Ishikawa *et al.*, *Development* **128**, 25 (2001).
23. A. M. Goodwin, J. Kitajewski, P. A. D'Amore, *Growth Factors* **25**, 25 (2007).
24. K. Venkiteswaran *et al.*, *Am. J. Physiol. Cell Physiol.* **283**, C811 (2002).
25. M. Wright, M. Aikawa, W. Szeto, J. Papkoff, *Biochem. Biophys. Res. Commun.* **263**, 384 (1999).
26. T. N. Masckauchan *et al.*, *Mol. Biol. Cell* **17**, 5163 (2006).
27. T. N. Masckauchan, C. J. Shawber, Y. Funahashi, C. M. Li, J. Kitajewski, *Angiogenesis* **8**, 43 (2005).
28. H. Yano *et al.*, *Neurol. Res.* **22**, 527 (2000).
29. H. Yano *et al.*, *Neurol. Res.* **22**, 650 (2000).

30. We thank P. D'Amore for helpful discussions. Supported by a Wenner-Gren Foundations (Sweden) postdoctoral fellowship (J.M.S.), National Heart, Lung, and Blood Institute grant HL076393 (J.R.), and NIH grant DK054364 (A.P.M.). The authors have a patent pending on the basis of the results reported in this paper. A.P.M. has been a paid consultant for Merck, Genentech, and Wythe in the past 3 years.

Supporting Online Material

www.sciencemag.org/cgi/content/full/322/5905/1247/DC1
Materials and Methods
Figs. S1 to S19
References

13 August 2008; accepted 6 October 2008
10.1126/science.1164594

Regulation of Pancreatic β Cell Mass by Neuronal Signals from the Liver

Junta Imai,[1] Hideki Katagiri,[2]* Tetsuya Yamada,[1] Yasushi Ishigaki,[1] Toshinobu Suzuki,[1,2] Hirohito Kudo,[1,2] Kenji Uno,[2] Yutaka Hasegawa,[1] Junhong Gao,[2] Keizo Kaneko,[1,2] Hisamitsu Ishihara,[1] Akira Niijima,[3] Masamitsu Nakazato,[4] Tomoichiro Asano,[5] Yasuhiko Minokoshi,[6] Yoshitomo Oka[1]

Metabolic regulation in mammals requires communication between multiple organs and tissues. The rise in the incidence of obesity and associated metabolic disorders, including type 2 diabetes, has renewed interest in interorgan communication. We used mouse models to explore the mechanism whereby obesity enhances pancreatic β cell mass, pathophysiological compensation for insulin resistance. We found that hepatic activation of extracellular regulated kinase (ERK) signaling induced pancreatic β cell proliferation through a neuronal-mediated relay of metabolic signals. This metabolic relay from the liver to the pancreas is involved in obesity-induced islet expansion. In mouse models of insulin-deficient diabetes, liver-selective activation of ERK signaling increased β cell mass and normalized serum glucose levels. Thus, interorgan metabolic relay systems may serve as valuable targets in regenerative treatments for diabetes.

Obesity is a major public health concern in most industrialized countries (*1*). The development of insulin resistance in obese individuals can promote pancreatic β cell proliferation, a compensatory response that leads to increased insulin secretion (*2*). This in turn can lead to hyperinsulinemia, often observed in type 2 diabetes and metabolic syndrome. The mechanism(s) by which obesity-induced insulin resistance alters pancreatic β cell mass are poorly understood.

Metabolic communication between organs is essential for maintaining systemic glucose and energy homeostasis. In addition to humoral factors such as hormones and cytokines (*3*, *4*), neuronal signals, both afferent (*5*, *6*) and efferent (*7*), play important roles in such interorgan metabolic communication (*8*). Disruption of insulin signaling in the liver (*9*), but not in muscle (*10*) or adipose tissue (*11*), induces pancreatic β cell hyperplasia and hyperinsulinemia, which suggests that the liver plays important roles in regulating pancreatic β cell mass.

To identify possible mechanisms underlying the compensatory responses of pancreatic β cells to obesity-induced insulin resistance, we studied proteins that are up-regulated or activated in the livers of mouse obesity models. One of these proteins is extracellular regulated kinase (ERK). We confirmed that ERK phosphorylation is enhanced in the livers of leptin-deficient (ob/ob) and high-fat-diet–induced obese (HF) mice (fig. S1A) (*12*), two murine obesity models that exhibit islet hyperplasia in response to insulin resistance.

Activation of mitogen-activated protein kinase/ERK kinase (MEK) results in ERK phosphorylation (*13*). To elucidate the metabolic roles of hepatic ERK activation, we expressed the constitutively active mutant of MEK-1 (CAM) in the liver (*14*). To distinguish endogenous from exogenous MEK1, we expressed the *Xenopus* homolog of MEK1. Mice administered an adenovirus encoding the LacZ gene were used as controls. Systemic infusion of recombinant adenoviruses resulted in expression of transgenes primarily in the liver, particularly hepatocytes (*6*) (fig. S1B), with no detectable expression in other organs, including the gastrointestinal tract (fig. S1C). Hepatic ERK phosphorylation, which is dependent on adenoviral titers (fig. S1D), was strongly enhanced on day 3 but had returned to the control level by day 9 after adenoviral administration (Fig. 1A). Hepatic ERK phosphorylation levels of CAM mice on day 3 were at most 2.1 times as high as those in the murine obesity model (fig. S1A). Hepatic lipid accumulation was markedly enhanced on day 3 but had also returned to the control level by day 14 (fig. S1E). No tumor formation was observed in the livers of CAM mice on day 44 (fig. S1F).

[1]Division of Molecular Metabolism and Diabetes, Tohoku University Graduate School of Medicine, Sendai 980-8575, Japan. [2]Division of Advanced Therapeutics for Metabolic Diseases, Center for Translational and Advanced Animal Research, Tohoku University Graduate School of Medicine, Sendai 980-8575, Japan. [3]Niigata University School of Medicine, Niigata 951-8150, Japan. [4]Third Department of Internal Medicine, Miyazaki Medical College, University of Miyazaki, Kiyotake, Miyazaki 889-1692, Japan. [5]Department of Medical Science, Graduate School of Medicine, University of Hiroshima, Hiroshima, Japan. [6]Division of Endocrinology and Metabolism, Department of Developmental Physiology, National Institute for Physiological Sciences, Okazaki, Japan.

*To whom correspondence should be addressed. E-mail: katagiri@mail.tains.tohoku.ac.jp

Notably, CAM-adenovirus administration induced insulin hypersecretion. CAM mice exhibited better glucose tolerance, with markedly higher serum insulin levels at 15 min after a glucose load during glucose tolerance testing (Fig. 1B) but no significant alterations in insulin sensitivity (Fig. 1C). Enhanced glucose-stimulated insulin secretion was also observed in isolated pancreatic islets from CAM mice (fig. S2A). Hepatic expression levels of gluconeogenic enzymes were decreased in CAM mice (fig. S2B), which may account for the lowering of fasting blood glucose levels. In addition, pancreatic islet masses in CAM mice increased gradually, by a factor of 1.9 on day 15 (Fig. 1D and fig. S2C), with no significant differences in the body weights of LacZ and CAM mice (fig. S2D). The pancreatic insulin content of CAM mice also increased, rising to more than double the control level on day 16 (Fig. 1E), although these insulinotropic effects were attenuated after about 6 weeks (fig. S3, A and B). Hepatic activation of the p38 MAPK pathway—another MAPK pathway induced by administration of adenovirus encoding the constitutively active mutant of MAPK kinase 6 (CAMKK6) (fig. S4A)—did not cause insulin hypersecretion (fig. S4B) or increase pancreatic insulin content (fig. S4C).

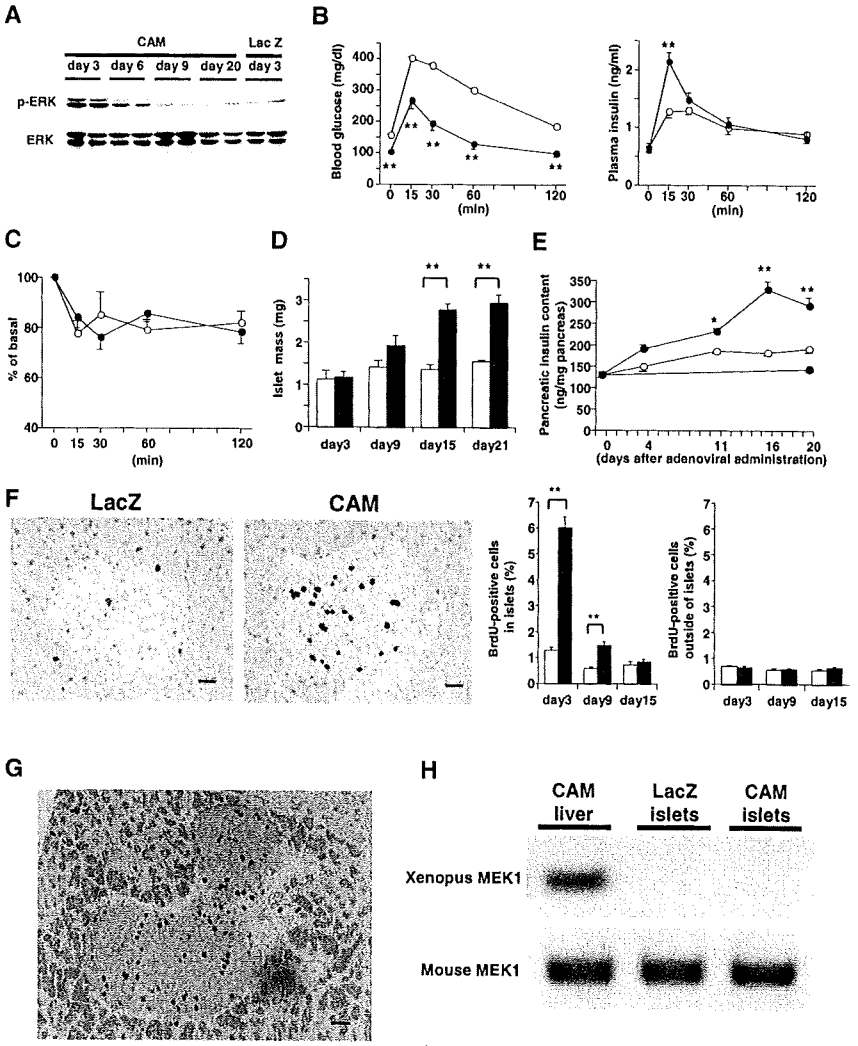

Fig. 1. Activation of hepatic ERK pathway in mice enhances glucose-stimulated insulin secretion and pancreatic β cell proliferation. **(A)** Time courses of hepatic ERK phosphorylation after injection of 1×10^8 plaque-forming units (PFU) per mouse of recombinant adenovirus containing CAM. **(B)** Blood glucose (left) and plasma insulin (right) levels during glucose tolerance tests performed on day 3 after adenoviral administration. **(C)** Blood glucose levels after intraperitoneal insulin injection on day 3 after adenoviral administration. Data are presented as percentages of the blood glucose levels immediately before insulin loading. In (B) and (C), open and closed circles indicate LacZ and CAM mice, respectively. **(D and E)** Time course of islet masses (D) and pancreatic insulin content (E). In (E), white, gray, and black circles indicate LacZ, CAM and untreated mice, respectively. **(F)** BrdU staining of pancreases. Representative images on day 3 after adenoviral administration are shown in the two left panels. Scale bar, 100 μm. Time course of BrdU-positive cell ratios within (left) and outside of (right) the islets. In (D) and (F), open and closed bars indicate LacZ and CAM mice, respectively. **(G)** Double staining of pancreases from CAM mice with BrdU (brown) and insulin (red) on day 3 after adenoviral administration. A representative image is shown. Scale bar, 100 μm. **(H)** Expression of exogenous (*Xenopus*) MEK1 (upper panel) and endogenous (mouse) MEK1 (lower panel) in pancreatic islets of LacZ and CAM mice on day 3 after adenoviral treatments. After 40 polymerase chain reaction cycles, the samples were subjected to gel electrophoresis. Data are presented as means ± SEM. *, $P < 0.05$, **, $P < 0.01$ versus LacZ mice, assessed by unpaired *t* test.

The ERK pathway in pancreatic β cells is required for mitogenic responses (*15*); however, exogenous *Xenopus* MEK1 expression was undetectable in CAM mouse islets (Fig. 1H), making it unlikely that the β cell proliferation observed in CAM mice is due to direct infection of pancreatic β cells by the CAM-adenovirus.

We hypothesized that interorgan metabolic communication from the liver to pancreatic islets is the mechanism underlying insulin hypersecretion and selective proliferation of pancreatic β cells in CAM mice. Efferent vagal signals to the pancreas modulate insulin secretion (*16*) and pancreatic islet mass (*17*, *18*). To examine the possible role of efferent vagal signals, we performed pancreatic vagotomy (PV) or a sham operation on the mice, followed by adenoviral administration 7 days later. PV almost completely abolished the CAM-induced glucose-lowering effects (Fig. 2A) and enhancement of glucose-stimulated insulin secretion (Fig. 2B), as well as the increases in pancreatic insulin content (Fig. 2C) and BrdU-positive islet cells (Fig. 2D) with no significant body weight alterations (fig. S5A). PV did not decrease glucose-stimulated insulin secretion, pancreatic insulin contents, or BrdU-positive islet cell numbers in LacZ mice (Fig. 2, B to D). These results strongly suggest that vagal nerves innervating the pancreas are involved in insulin hypersecretion and pancreatic β cell proliferation in CAM mice.

Thus, hepatic ERK activation is likely to transmit signals from the liver to the central nervous system (CNS), resulting in activation of the efferent vagus to the pancreas. To explore afferent signals from the liver to the CNS, we first performed hepatic vagotomy (HV). Contrary to the PV results, however, HV did not affect blood glucose levels (Fig. 2A), glucose-stimulated insulin secretion (Fig. 2B), or pancreatic insulin content (Fig. 2C) in CAM mice. Next, we blocked another type of afferent neuronal signal originating in the liver, the splanchnic nerve, which contains

afferent fibers from the hepatobiliary system (*19*). Capsaicin application to the splanchnic nerve caused selective pharmacological deafferentation with no apparent effects on other nerves, including subdiaphragmatic vagal trunks (fig. S5B), and markedly blunted the glucose-lowering effects (Fig. 2E), glucose-stimulated insulin secretion (Fig. 2F), and increases in pancreatic insulin content (Fig. 2G) and BrdU-positive islet cells (Fig. 2H) in CAM mice. To exclude the possibility that these capsaicin effects are mediated by blockade of the celiac branch of the vagal nerve, we performed denervation of the celiac branch in CAM mice. After celiac vagus dissection, CAM-adenovirus administration still increased glucose-stimulated insulin secretion during glucose tolerance testing (fig. S6A) and pancreatic insulin content (fig. S6B). Collectively, these results suggest afferent signals from the liver to the CNS to be at least partially mediated by afferent splanchnic nerves.

To evaluate CNS involvement, we performed bilateral midbrain transection (MBT), which was confirmed by functional (fig. S7A) and histological (fig. S7B) analyses. MBT markedly blunted the glucose-lowering effects (Fig. 2I), glucose-stimulated insulin secretion (Fig. 2J), and increase in pancreatic insulin content (Fig. 2K) in CAM mice, suggesting CNS involvement in this neuronal pathway. Thus, the mechanism underlying these selective islet responses observed in CAM

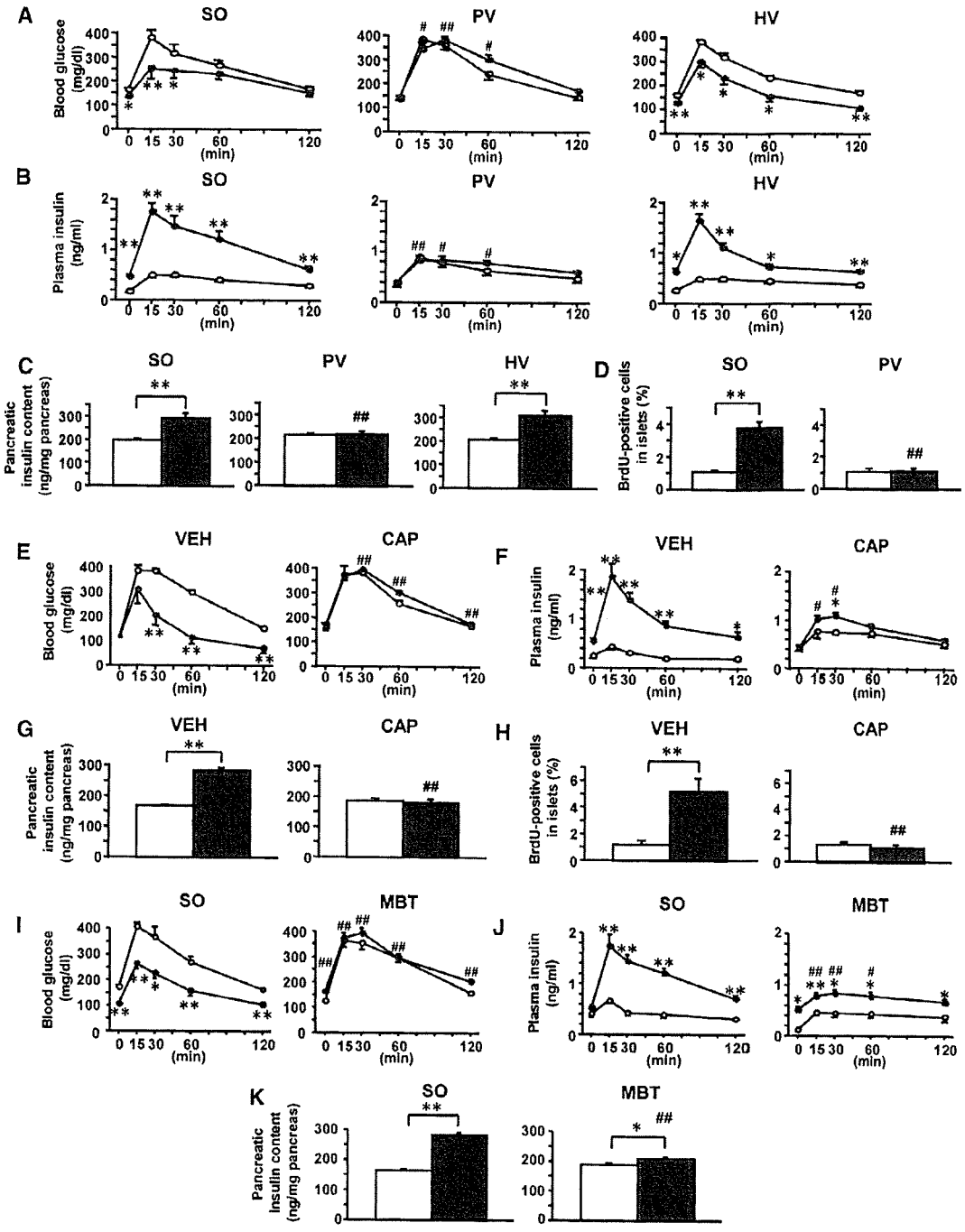

Fig. 2. Dissection of the pancreatic vagus, afferent blockade of the hepatic splanchnic nerve, or midbrain transection inhibits pancreatic β cell proliferation and insulin hypersecretion in CAM mice. (**A** and **B**, **E** and **F**, and **I** and **J**) Blood glucose [(A), (E), and (I)] and plasma insulin [(B), (F), and (J)] levels during glucose tolerance tests performed on day 3 after adenoviral administration, after sham operation (SO), pancreatic vagotomy (PV), and hepatic vagotomy (HV) [(A) and (B)], vehicle (VEH) and capsaicin (CAP) treatments [(E) and (F)], and SO and midbrain transection (MBT) [(I) and (J)]. (**C**, **G**, and **K**) Pancreatic insulin content of SO, PV and HV mice (C), VEH and CAP mice (G), and SO and MBT mice (K) on day 16 after adenoviral administration. (**D** and **H**) BrdU-positive cell ratios in whole islet cells in SO and PV mice (D) and VEH and CAP mice (H) on day 3 after adenoviral administration. Open bars/circles, LacZ mice; closed bars/circles, CAM mice. Data are presented as means ± SEM. *, $P < 0.05$; **, $P < 0.01$ versus LacZ mice; #, $P < 0.05$; ##, $P < 0.01$ versus SO-CAM [(A) to (D) and (I) to (K)] or VEH-CAM [(E) to (H)] mice, assessed by unpaired *t* test.

mice involves interorgan communication mediated by the peripheral and the central nervous system.

To determine whether this neuronal interorgan communication is involved in islet hyperplasia in obesity-induced insulin resistance, we inhibited hepatic hyperactivation of ERK signaling (fig. S1A) by expressing the dominant-negative mutant of MEK1 (DNM) in the livers of ob/ob and HF obesity mice. DNM-adenovirus administration suppressed hepatic ERK phosphorylation (Fig. 3A and fig. S8A) without affecting hepatic p38 MAPK phosphorylation (fig. S4D). In LacZ-adenovirus–treated control ob/ob and HF mice, pancreatic insulin content rose significantly, paralleling obesity development. In contrast, DNM-adenovirus administration blunted these rises in pancreatic insulin content in ob/ob (Fig. 3B) and HF mice (fig. S8B). These findings suggest that activation of the hepatic ERK pathway is involved in pancreatic islet expansion during obesity development.

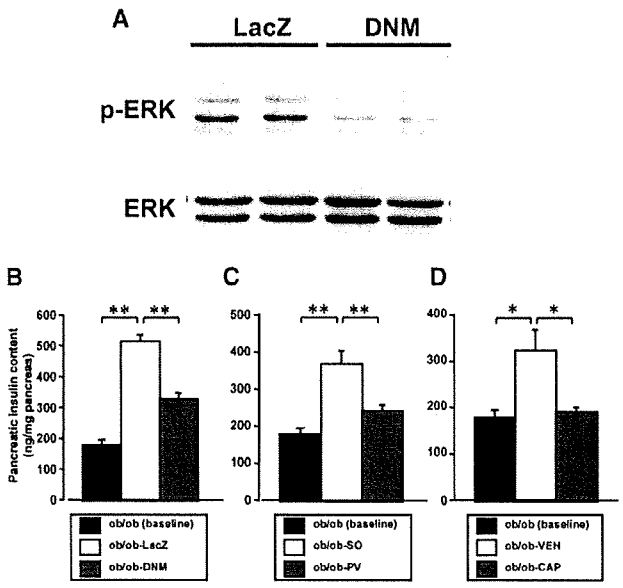

Fig. 3. The interorgan communication system originating in the liver is involved in compensatory islet expansion in response to insulin resistance associated with obesity. **(A)** Hepatic ERK phosphorylation in ob/ob mice on day 7 after administration of 5×10^8 PFU per mouse of recombinant adenovirus containing LacZ or the dominant-negative mutant of the MEK1 (DNM) gene. **(B)** Pancreatic insulin content of ob/ob mice on day 8 after LacZ (white bar) or DNM (gray bar) adenovirus administration. **(C** and **D)** Pancreatic insulin content before and after denervation experiments. Pancreatic insulin content of ob/ob mice on day 14 after SO (white bar) or PV (gray bar) (C) and on day 21 after VEH (white bar) or CAP (gray bar) treatment (D). In (B) to (D), pancreatic insulin content of 5-week-old ob/ob mice were used as baseline controls (black bars). *, $P < 0.05$; **, $P < 0.01$ versus LacZ-adenovirus–treated (B), SO (C) or VEH (D) ob/ob mice, assessed by unpaired t test. Data are presented as means ± SEM.

To determine whether targeting of this interorgan communication system affects insulin-deficient (type 1) diabetes, we administered CAM-adenovirus to streptozotocin (STZ)–induced diabetic mice, a murine model of pharmacological β cell loss. Fasting blood glucose levels of CAM-adenovirus–treated STZ mice were dramatically improved (Fig. 4A). This was associated with an increase in the number of BrdU-positive islet cells (Fig. 4B) and an increase in pancreatic insulin content (Fig. 4C). We then administered CAM-adenovirus to Akita mice (*20*), a murine model of endoplasmic reticulum (ER) stress–induced β cell loss (*21*), because ER stress in β cells is involved in diabetes development (*22–24*). In these mice as well, CAM-adenovirus treatment lowered blood glucose levels (Fig. 4D), enhanced proliferation of pancreatic islet cells (Fig. 4E), and increased pancreatic insulin content (Fig. 4F). In both these mouse models of insulin-deficient diabetes, CAM-adenovirus treatment greatly improved glucose tolerance by raising serum insulin levels (fig. S9, A and C) but did not significantly alter insulin sensitivity (fig. S9, B and D). In STZ-induced diabetic mice, the glucose-lowering effect induced by CAM persisted for at least 38 days (Fig. 4A), although in Akita mice it was gradually attenuated and was no longer significant by day 36 (Fig. 4D), possibly due to ER stress–induced apoptosis of regenerated β cells. Thus, manipulation of this interorgan communication system may lead to the development of novel therapeutic strategies for insulin-deficient diabetes.

We have identified a neuronal relay that induces proliferation of pancreatic β cells in response to insulin resistance, indicating that the CNS obtains information from peripheral organs and mod-

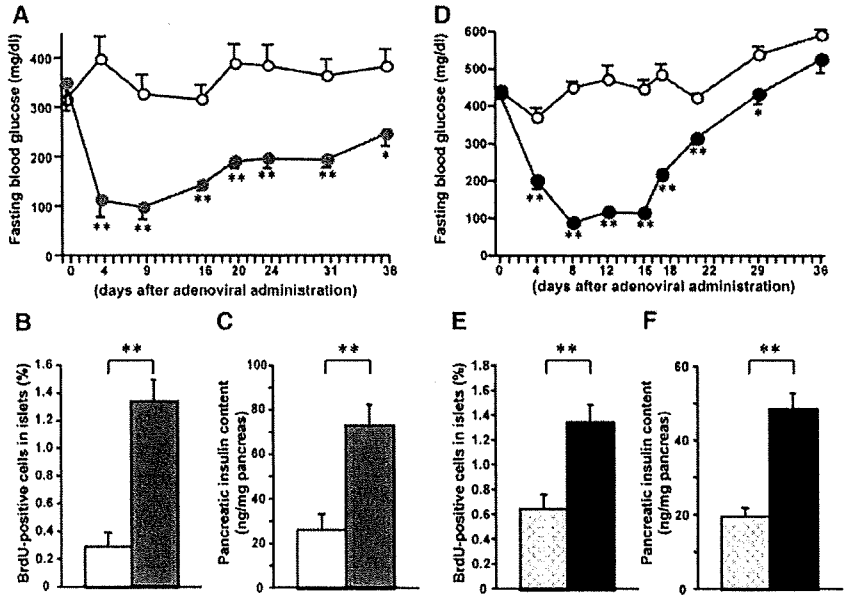

Fig. 4. Hepatic ERK activation induces pancreatic β cell proliferation and normalizes blood glucose levels in murine models of insulin-deficient diabetes. **(A** and **D)** Time course of fasting blood glucose levels in 1.5×10^8 PFU per mouse of LacZ- and CAM-adenovirus–treated STZ (A) and Akita (D) mice. **(B** and **E)** BrdU-positive cell ratios in whole islet cells in STZ-LacZ and STZ-CAM mice (B) and Akita-LacZ and Akita-CAM mice (E) on day 3 after adenoviral administration. **(C** and **F)** Pancreatic insulin content of STZ-LacZ and STZ-CAM mice (C) and Akita-LacZ and Akita-CAM mice (F) on day16 after adenoviral administration. (A) to (C): white bars/circles, STZ-LacZ mice; gray bars/circles, STZ-CAM mice. (D) to (F): dotted bars/circles, Akita-LacZ-mice; black bars/circles, Akita-CAM-mice. Data are presented as means ± SEM. *, $P < 0.05$; **, $P < 0.01$ versus [(A) to (C)] STZ-LacZ mice or [(D) to (F)] Akita-LacZ mice, assessed by unpaired t test.

ulates pancreatic islet mass. Hepatic ERK activation is likely to play an important role in compensatory islet hyperplasia, although it is not yet clear how ERK signaling affects the neuronal pathway. The therapeutic effects we observed in two mouse models of insulin-deficient diabetes are especially noteworthy. Type 1 diabetes mellitus is characterized by progressive loss of pancreatic β cells, leading to a life-long insulin dependency. Recently, it was reported that β cell mass is also decreased in type 2 diabetes (*25*). Although substantial progress has been made with therapies that are based on transplantation of pancreatic islets (*26*), immune rejection and donor supply are still major challenges. In this context, therapeutic manipulation of the interorgan signaling mechanism described here may merit investigation as a potential strategy for regeneration of a patient's own β cells. Our results may open a new paradigm for regenerative medicine: regeneration of damaged tissues by targeting of interorgan communication systems, especially neural pathways.

References and Notes

1. J. P. Despres, I. Lemieux, *Nature* **444**, 881 (2006).
2. M. Prentki, C. J. Nolan, *J. Clin. Invest.* **116**, 1802 (2006).
3. J. M. Friedman, J. L. Halaas, *Nature* **395**, 763 (1998).
4. E. D. Rosen, B. M. Spiegelman, *Nature* **444**, 847 (2006).
5. T. Yamada *et al.*, *Cell Metab.* **3**, 223 (2006).
6. K. Uno *et al.*, *Science* **312**, 1656 (2006).
7. T. K. Lam, G. J. Schwartz, L. Rossetti, *Nat. Neurosci.* **8**, 579 (2005).
8. H. Katagiri, T. Yamada, Y. Oka, *Circ. Res.* **101**, 27 (2007).
9. M. D. Michael *et al.*, *Mol. Cell* **6**, 87 (2000).
10. J. C. Bruning *et al.*, *Mol. Cell* **2**, 559 (1998).
11. M. Bluher *et al.*, *Dev. Cell* **3**, 25 (2002).
12. S. Yang, H. Z. Lin, J. Hwang, V. P. Chacko, A. M. Diehl, *Cancer Res.* **61**, 5016 (2001).
13. L. Chang, M. Karin, *Nature* **410**, 37 (2001).
14. Materials and methods are available as supporting material on *Science* Online.
15. R. K. Gupta *et al.*, *Genes Dev.* **21**, 756 (2007).
16. D. Gautam *et al.*, *Cell Metab.* **3**, 449 (2006).
17. T. Kiba *et al.*, *Gastroenterology* **110**, 885 (1996).
18. A. Edvell, P. Lindstrom, *Am. J. Physiol.* **274**, E1034 (1998).
19. H. R. Berthoud, *Anat. Rec. A Discov. Mol. Cell. Evol. Biol.* **280**, 827 (2004).
20. J. Wang *et al.*, *J. Clin. Invest.* **103**, 27 (1999).
21. S. Oyadomari *et al.*, *J. Clin. Invest.* **109**, 525 (2002).
22. H. P. Harding, D. Ron, *Diabetes* **51** (suppl. 3), S455 (2002).
23. R. J. Kaufman, *J. Clin. Invest.* **110**, 1389 (2002).
24. H. Ishihara *et al.*, *Hum. Mol. Genet.* **13**, 1159 (2004).
25. A. E. Butler *et al.*, *Diabetes* **52**, 102 (2003).
26. A. M. Shapiro *et al.*, *New Engl. J. Med.* **355**, 1318 (2006).

27. We thank M. Yokoyama for the generous gift of recombinant adenoviruses. This work was supported by Grants-in Aid (H.K., Y.O., and J.I.); the 21st Center of Excellence (COE) (H.K.) and Global-COE (Y.O.) programs from the Ministry of Education, Culture, Sports, Science and Technology of Japan; and a Grant-in Aid (Y. O.) from the Ministry of Health, Labor and Welfare of Japan. Tohoku University, J. I., H.K., and Y.O have applied for patents related to this work in the United States and Japan.

Supporting Online Material

www.sciencemag.org/cgi/content/full/322/5905/1250/DC1
Materials and Methods
Figs. S1 to S9
References

5 February 2008; accepted 15 October 2008
10.1126/science.1163971

Control of Toxic Marine Dinoflagellate Blooms by Serial Parasitic Killers

Aurelie Chambouvet, Pascal Morin, Dominique Marie, Laure Guillou*

The marine dinoflagellates commonly responsible for toxic red tides are parasitized by other dinoflagellate species. Using culture-independent environmental ribosomal RNA sequences and fluorescence markers, we identified host-specific infections among several species. Each parasitoid produces 60 to 400 offspring, leading to extraordinarily rapid control of the host's population. During 3 consecutive years of observation in a natural estuary, all dinoflagellates observed were chronically infected, and a given host species was infected by a single genetically distinct parasite year after year. Our observations in natural ecosystems suggest that although bloom-forming dinoflagellates may escape control by grazing organisms, they eventually succumb to parasite attack.

Although photosynthetic dinoflagellates are important primary producers in marine ecosystems, some bloom-forming species produce toxins that can cause illness and even death in humans (*1*). These harmful algal blooming (HAB) species are particularly prevalent in warm, stratified, and nutrient-enriched coastal waters (*2*, *3*). Documented HAB events have increased substantially during recent decades as a result of extensive coastal eutrophication and, possibly, global climate change (*4*).

In 1968, Taylor proposed using specific dinoflagellate parasites, such as the Syndiniales *Amoebophrya* spp. (*5*), as biological control agents for HAB organisms. This idea was rejected because of the apparent lack of specificity of the parasites; however, the homogeneous morphology of these parasites masks extensive genetic diversity (*6*). Recently, the widespread existence of *Amoebophrya* spp. was "rediscovered" by culture-independent methods, and they were renamed "novel alveolate group II" (*7*–*9*). This eukaryotic lineage frequently forms 10 to 50% of sequences retrieved within coastal environmental clone libraries (*10*, *11*). Indeed, up to 44 distinct clusters have been detected, with extensive intraclade genetic diversity (*12*); the genetic diversity of the parasites appears to be comparable to the species richness of their hosts.

We sampled a marine coastal estuary (the Penzé River, northern Brittany, France) for 3 consecutive years (2004 to 2006), using catalyzed reporter deposition fluorescent in situ hybridization (CARD-FISH; tables S1 and S2) with probes specifically designed to detect group II alveolates. Our aim was to examine how the abundance and diversity of the parasites influenced their host populations in natural environments. In May and June of each year, we observed a rapid succession of four major species of photosynthetic

Table 1. Specificity of Syndiniales group II in the Penzé estuary in 2005 and 2006. Prevalences (percentage of infected cells) when a general oligonucleotide probe (ALV01) and clade-specific probes were used are shown (results for clades 1, 2, and 14; for description of clades see Fig. 3). Observations of a mature trophont inside the host cell are indicated by an asterisk. ND, not done. Numbers in parentheses show the percentage of the signal obtained when the general probe was used, explained by the clade-specific probes.

Host species	Dates (day/month/year)	Syndiniales group II, all clades	Syndiniales group II, clade 1	Syndiniales group II, clade 2	Syndiniales group II, clade 14
H. rotundata	03/06/2005	26*	26* (100%)	ND	ND
	29/05/2006	29*	23* (79%)	0	2 (<1%)
S. trochoidea	14/06/2005	23*	ND	11* (48%)	ND
	16/06/2006	33*	0	18* (55%)	3 (<1%)
	18/06/2006	26*	0	29* (>100%)	9 (3%)
A. minutum	14/06/2005	40*	0	0	0
	22/06/2006	19*	6 (3%)	0	0
H. triquetra	20/06/2005	10*	ND	0	11* (>100%)
	22/06/2006	14*	0	0	14* (100%)

Station Biologique, CNRS, UMR 7144, Place Georges Teissier, 29682 Roscoff Cedex, France; and Laboratoire Adaptation et Diversité en Milieu Marin, Université Pierre et Marie Curie, Paris 6, Paris, France.

*To whom correspondence should be addressed. E-mail: lguillou@sb-roscoff.fr

ELSEVIER

Atherosclerosis 196 (2008) 391–397

ATHEROSCLEROSIS

www.elsevier.com/locate/atherosclerosis

A novel method for evaluating human carotid artery elasticity: Possible detection of early stage atherosclerosis in subjects with type 2 diabetes

Hisashi Okimoto[a,1], Yasushi Ishigaki[a,1], Yoshihiro Koiwa[b], Yoshinori Hinokio[a], Takehide Ogihara[c], Susumu Suzuki[a], Hideki Katagiri[c,f], Takayoshi Ohkubo[d,f], Hideyuki Hasegawa[e], Hiroshi Kanai[e], Yoshitomo Oka[a,g,*]

[a] *Division of Molecular Metabolism and Diabetes, Tohoku University Graduate School of Medicine, Japan*
[b] *Division of Cardiovascular Medicine, Tohoku University Graduate School of Medicine, Japan*
[c] *Division of Advanced Therapeutics for Metabolic Diseases, Tohoku University Graduate School of Medicine, Japan*
[d] *Department of Planning for Drug Development and Clinical Evaluation, Tohoku University Graduate School of Pharmaceutical Science and Medicine, Japan*
[e] *Department of Electrical Engineering, Tohoku University Graduate School of Engineering, Japan*
[f] *The 21st Century COE Programs, Comprehensive Research and Education Center for Planning of Drug Development and Clinical Evaluation, Japan*
[g] *The 21st Century COE Programs, Center for Innovative Therapeutic Development towards the Conquest of Signal Transduction Diseases, Tohoku University, Sendai, Japan*

Received 29 March 2006; received in revised form 5 September 2006; accepted 12 November 2006
Available online 18 December 2006

Abstract

We recently developed a novel method for evaluating the elasticity of arterial walls, the phased tracking method. Herein, we evaluated atherosclerosis of the carotid artery with this method in 242 individuals with type 2 diabetes. In multiple regression analysis of subject status, age, systolic blood pressure and hyperlipidemia were found to be independently associated with carotid artery elasticity values. We also measured currently established values for atherosclerosis, carotid artery IMT and baPWV, in these subjects. Carotid artery elasticity correlated with max IMT ($r=0.291$, $p<0.01$), plaque score (PS) ($r=0.220$, $p<0.01$) and baPWV ($r=0.345$, $p<0.01$). Elasticity, max IMT and plaque score, all correlated with the number of risk factors for atherosclerosis, i.e. hypertension, hyperlipidemia and smoking, in addition to diabetes, consistent with the view that these values reflect atherosclerosis. Importantly, however, in subjects with IMT <1.1 mm, who are classified as not having atherosclerosis as defined by IMT criteria, only carotid artery elasticity correlated with the number of risk factors ($p<0.05$). These results suggest that (1) the measured carotid artery elasticity values reflect atherosclerosis and (2) our novel method has potential for detecting atherosclerosis in its early stage.

Keywords: Human carotid artery elasticity; Atherosclerosis; Diabetes

1. Introduction

Individuals with type 2 diabetes are at very high risk for atherosclerosis [1]. Although many methods have been developed for detecting atherosclerosis, those currently available are mainly for detecting established atherosclerosis. Therefore, the disease process is well-advanced at the time of diagnosis. To reduce future cardiovascular complications in subjects with atherogenic disorders such as type 2 diabetes

* Corresponding author at: Division of Molecular Metabolism and Diabetes, Tohoku University Graduate School of Medicine, 2-1 Seiryo-machi, Aoba-ku, Sendai 980-8575, Japan. Tel.: +81 22 717 7611; fax: +81 22 717 7611.
E-mail address: oka-y@mail.tains.tohoku.ac.jp (Y. Oka).
[1] These authors contributed equally to this work.

0021-9150/$ – see front matter © 2006 Elsevier Ireland Ltd. All rights reserved.
doi:10.1016/j.atherosclerosis.2006.11.020

mellitus, detection of early stage atherosclerosis is urgently needed.

Carotid intima-media thickness (IMT) is a well-established surrogate marker for cardiovascular risk [2]. Measuring IMT with ultrasonography is non-invasive and relatively simple [3,4], and IMT is now commonly employed as an endpoint marker in clinical trials. Carotid IMT correlates with cardiovascular risk factors and indeed predicts macrovascular events such as myocardial infarction [5] and stroke [6]. Carotid IMT is greater in subjects with diabetes, both type 1 [7] and type 2 [8,9], than in non-diabetic subjects of the same age. When analyzed in diabetic patients, IMT correlates with glycemic control and the duration of diabetes. Interventions, such as blood glucose lowering [10], lipid lowering [11], ACE inhibition [12] and anti-platelet treatment [13], have been demonstrated to suppress IMT progression. However, it has also been reported that IMT is not affected by either therapeutic interventions [14] or glycemic control [15]. These conflicting results might be attributable to a very small change in IMT, a 0.1 mm increase per decade in normal subjects. Such a small change may mask actual change due to inter-assay variations in IMT measurement. Most importantly, it is not possible to make a diagnosis of atherosclerosis until the appearance of arterial wall thickening.

We recently developed a novel non-invasive method for evaluating the movement of multiple sites in cardiac and arterial walls (3.616 measurement sites/9.0 mm × 6.4 mm) during a single heartbeat [16,17]. This innovative phased tracking method enables us to evaluate regional characteristics; the softer the site, the more easily it deforms during one heartbeat. This reflects regional elasticity. This method has already been applied to the in vivo detection of regional changes in cardiac and arterial walls [18–20], and the interventricular septum [21]. Evaluation of plaque vulnerability has also been attempted [16]. It is theoretically possible to detect qualitative changes in the carotid arterial wall with this method. We therefore tested the possibility of being able to detect atherosclerosis in the early stage.

Herein, we show that carotid artery elasticity, as measured in Japanese subjects with type 2 diabetes, correlates well with results obtained with currently established methods for evaluating atherosclerosis. Most importantly, elasticity correlates with the number of risk factors for atherosclerosis in those with IMT <1.1 mm, who are classified as not having atherosclerosis as defined by IMT criteria [22,23]. These results strongly suggest that it is possible to detect early stage atherosclerosis with this novel method.

2. Methods

2.1. Study subjects

The study subjects were recruited from among patients followed at the diabetes clinic at Tohoku University Hospital. Patients with type 1 diabetes, renal failure (serum creatinine >2.0 mg/dl), severe heart failure (NYHA functional class 2–4), atrial fibrillation and peripheral arterial disease were excluded from the study. All participants analyzed were Japanese type 2 diabetes patients ($n=242$) who met the WHO criteria for diabetes mellitus. The study protocol was approved by the Tohoku University Institutional Review Board. Informed consent was obtained from each patient. Subjects characteristics are shown in Table 1.

Table 1
Subject characteristics

Number	242
Age (years)	62.1 ± 12.4
Male (%)	54.1
Body weight (kg)	62.2 ± 13.6
BMI (kg/m^2)	24.2 ± 4.2
Duration of diabetes (years)	12.0 ± 9.70
Fasting blood glucose (mg/dl)	141 ± 32.1
HbA1c (%)	7.08 ± 1.33
Systolic blood pressure (mmHg)	130 ± 18.3
Diastolic blood pressure (mmHg)	75.8 ± 11.1
Total cholesterol (mg/dl)	191 ± 38.4
HDL cholesterol (mg/dl)	51.2 ± 14.6
LDL cholesterol (mg/dl)	115 ± 31.9
Triglyceride (mg/dl)	127 ± 94.1
Uric acid (mg/dl)	5.09 ± 1.37
High-sensitive CRP (mg/dl)	0.18 ± 0.23
Diabetic retinopathy (%)	30.2
Microalbumiuria or proteinuria (%)	38.8
Diabetic neuropathy (%)	46.4
Diet:OHA:insulin (%)	20.0:37.8:42.2
Hyperlipidemia (%)	37.2
Hypertension (%)	39.3
Current smoker (%)	30.6
BMI >25 (%)	38.0

Data are presented as means ± S.D.

We used the following criteria for atherogenic risk factors. Hyperlipidemia was defined as total cholesterol ≥5.7 mmol/dl (220 mg/dl) and/or triglyceride ≥1.7 mmol/l (150 mg/dl), based on the definition proposed by the Japan Atherosclerosis Society in 2002, or taking antihyperlipidemic drugs. The subjects whose systolic BP ≥140 mmHg and/or diastolic BP ≥90 mmHg (The Japanese Society of Hypertension guidelines in 2004) or who were taking antihypertensive drugs were defined as having hypertension. The subjects who currently smoked were classified as current smokers.

2.2. Measurement of ABI and baPWV

Ankle brachial pressure index (ABI) and brachial ankle pulse wave velocity (baPWV) were measured using an automatic waveform analyzer (BP-203RPE; Colin Co., Komaki, Japan) after a 5 min rest. This device was designed to simultaneously measure blood pressure levels in both arms (brachial arteries) and ankles (posterior tibial arteries), and to then calculate the ankle systolic BP/brachial systolic BP. Pulse waves were recorded on the right brachial artery and both posterior tibial arteries. The average baPWV was calculated by divid-

ing the arm–ankle distance by the pulse wave transmission time between these points.

2.3. Measurement of carotid artery intima-media thickness

Intima-media thickness of the carotid arteries was measured using ultrasound diagnostic equipment (EUB-450, Hitachi Medico, Tokyo, Japan) with an electrical linear transducer (mid-frequency of 7.5 MHz). The common carotid artery (CCA), carotid bulb and portions of the internal and external carotid arteries on both sides were scanned with the subject in the supine position. The scan encompasses the region between 30 mm proximal to the beginning of the dilation of the bifurcation bulb and 15 mm distal to the CCA flow divider. We defined the max IMT as the thickest IMT in the scanned regions [24] and a max IMT <1.1 mm was considered normal. We defined a plaque, a focal IMT thickening, as an area with IMT $\geq$1.1 mm and calculated the plaque score (PS) by totaling the maximal thickness values of all plaques in the scanned area [25]. The scans were performed by a trained sonographer and the scanning period averaged 20 min in each patient.

2.4. Measurement of arterial wall elasticity

Real-time measurement of regional elasticity in the carotid artery wall was achieved based on a previously described method [20] with ultrasound diagnostic equipment (prototype system by Panasonic). With this system, an ultrasound beam is used for sequential scanning at 32 positions with a linear type 7.5 MHz probe. Multiple points were preset from the luminal surface to the adventitia along each beam with constant intervals of 320 μm, and multiple layers were defined as being between two neighboring points. Then, the displacement of each point preset along each beam was obtained by applying the phased tracking method to the received echo. Minute changes in the thickness of each layer were determined by subtracting displacements of two neighboring points. The elasticity of each layer was obtained from the thickness change and the blood pressure measured at the upper arm. Since the reflected ultrasound was resampled at an interval of 107 ns (=80 μm along the depth direction) after quadrature demodulation, we further divided each layer with a thickness of 320 μm into four points, shifted the initial depth of each layer by one-fourth of 320 μm, and applied the above procedure to each depth. Thus, the elasticity was obtained at intervals of 80 μm in the depth direction and 200 μm in the axial direction of the artery. A cross-sectional image and the process of elasticity measurement are schematically depicted in Fig. 1.

2.5. Statistical analysis

Variables were compared using Pearson's regression analysis and Student's *t*-test as appropriate. Then, a multiple linear regression analysis was performed to evaluate the independent parameters that were significantly related to arterial elasticity. The relationships between number of risk factors and the values of atherosclerosis markers were examined by analysis of covariance (ANCOVA), adjusted with age as a covariate. A p value less than 0.05 was accepted as indicating statistical significance. All statistical analyses were performed using the Statistical Package for the Social Sciences Version 13.0 (SPSS Japan Inc., Tokyo, Japan).

3. Results

We assessed the associations of carotid artery elasticity with subject characteristics (Table 2). Elasticity correlated

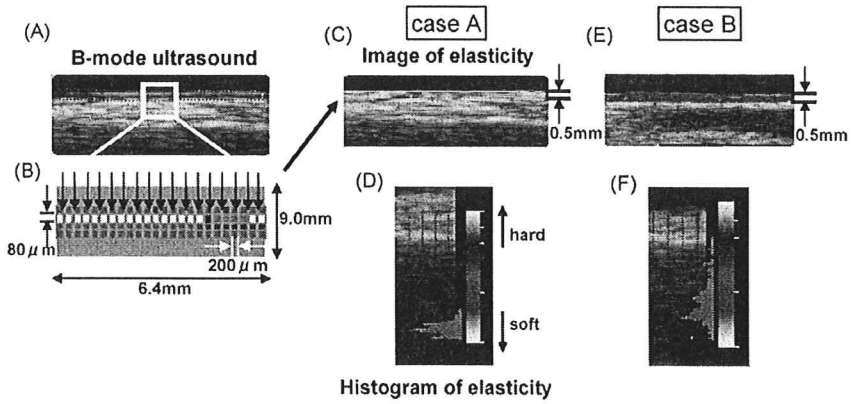

Fig. 1. The intima–media complex was visualized by conventional B-mode scanning (A), and minute thickness changes in the layers at each depth (113 depths × 32 beams per 9 mm × 6.4 mm scanned area) during one heart beat were then recorded by the phased tracking method (B). Thickness changes in each layer represent deformity, a reflection of elasticity. This elasticity is displayed as a 2D cross-sectional color image on B-mode scanning, and the image is updated at every heartbeat (C). The elasticity distribution is shown as a histogram (D). Representative results obtained from a normal subject, case A (male, age 40), are shown. Case B (male, age 45), in marked contrast, suffered from type 2 diabetes, hyperlipidemia and an old cerebral infarction, but had an IMT of only 0.5 mm, the same thickness as that of case A. The elasticity (E) was, however, extremely different from that of case A, as shown in the histogram (F).

Table 2
Associations between arterial elasticity and subject characteristics

Variables	r-Value	p-Value
Age	0.34	<0.01
Duration of diabetes	0.136	<0.05
Fasting blood glucose	−0.012	0.86
HbA1c	−0.003	0.97
Total cholesterol	0.103	0.10
HDL cholesterol	0.066	0.31
LDL cholesterol	0.089	0.17
Triglyceride	−0.064	0.32
Systolic blood pressure	0.443	<0.01
Diastolic blood pressure	0.147	<0.05
Uric acid	−0.03	0.65
High-sensitive CRP	0.037	0.56

Table 3
Mean arterial elasticity values in the presence and absence of cardiovascular risk factors

Variables	Elasticity (kPa)		p
	−	+	
Male	51.6 ± 12.6	51.0 ± 14.5	0.99
Hyperlipidemia	49.8 ± 12.3	54.7 ± 13.7	<0.01
Hypertension	49.6 ± 13.3	54.8 ± 13.6	<0.01
Current smoker	51.6 ± 13.3	51.8 ± 14.5	0.88
BMI >25	51.6 ± 13.7	51.6 ± 13.5	0.99
Diabetic retinopathy	52.3 ± 13.7	50.9 ± 14.1	0.67
Diabetic nephropathy	50.5 ± 13.6	53.9 ± 13.6	0.06
Diabetic neuropathy	50.8 ± 12.9	51.4 ± 14.4	0.65

Data are presented as means ± S.D.

Table 4
Multivariate adjustment for parameters related to arterial elasticity

Variables	Coefficient (β)	95% CI	p-Value
Age (years)	0.28	0.18–0.43	<0.01
Duration of diabetes (years)	−0.02	−0.18–0.14	0.77
Systolic blood pressure (mmHg)	0.39	0.21–0.38	<0.01
Hyperlipidemia	0.11	0.08–6.24	<0.05

with age ($r = 0.340$, $p < 0.01$), duration of diabetes ($r = 0.136$, $p < 0.05$) and blood pressure, both systolic ($r = 0.430$, $p < 0.01$) and diastolic ($r = 0.147$, $p < 0.05$).

We then examined whether or not cardiovascular risk factors affect arterial elasticity values (Table 3). Hyperlipidemic subjects had significantly higher arterial elasticity values than those with normal lipid profiles. Similarly, subjects with hypertension had higher values. However, arterial elasticity values did not depend on other risk factors, such as sex, obesity, smoking and diabetic complications.

To elucidate the independent variables affecting arterial elasticity, we performed multiple linear regression analysis with parameters related to elasticity. We employed four clinical parameters, age, duration of diabetes, systolic blood pressure and hyperlipidemia, based on the results shown in Tables 2 and 3. We found age, systolic blood pressure and hyperlipidemia to be independently associated with elasticity values (Table 4).

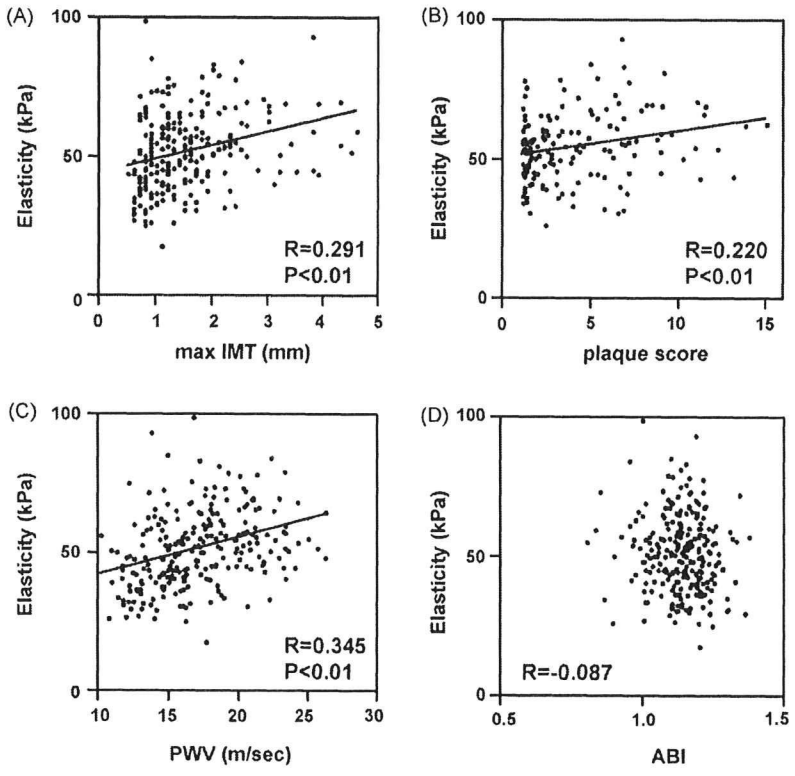

Fig. 2. Correlations between arterial elasticity values and max IMT (A), plaque score (B), baPWV (C) and ABI (D).

To assess the clinical relevance of carotid artery elasticity, we compared our elasticity values to those obtained with currently established methods for evaluating atherosclerosis: max IMT, plaque score, baPWV and ABI. Carotid artery elasticity showed significant positive correlations with max IMT ($r=0.291$, $p<0.01$) (Fig. 2A), the plaque score ($r=0.220$, $p<0.01$, $n=160$) (Fig. 2B) and baPWV ($r=0.345$, $p<0.01$) (Fig. 2C) in subjects with type 2 diabetes. It should be kept in mind that the plaque score can be obtained only in subjects with IMT ≥ 1.1 mm ($n=160$), such that the correlation was studied only in those having definite atherosclerosis based on IMT criteria [22,23]. Arterial elasticity showed no correlation with the ABI value ($r=-0.087$, $p=0.176$) (Fig. 2D). However, when we performed multiple linear regression analysis adjusted with independent parameters, age, systolic blood pressure and hyperlipidemia (Table 4), the correlations between elasticity and atherosclerosis markers (max IMT, plaque score and baPWV) were no longer present.

In a subject with more than one risk factor, the atherosclerotic process would be accelerated and thus affect the values of atherosclerosis markers. Four modifiable risk factors, diabetes, hypertension, hyperlipidemia and current smoking,

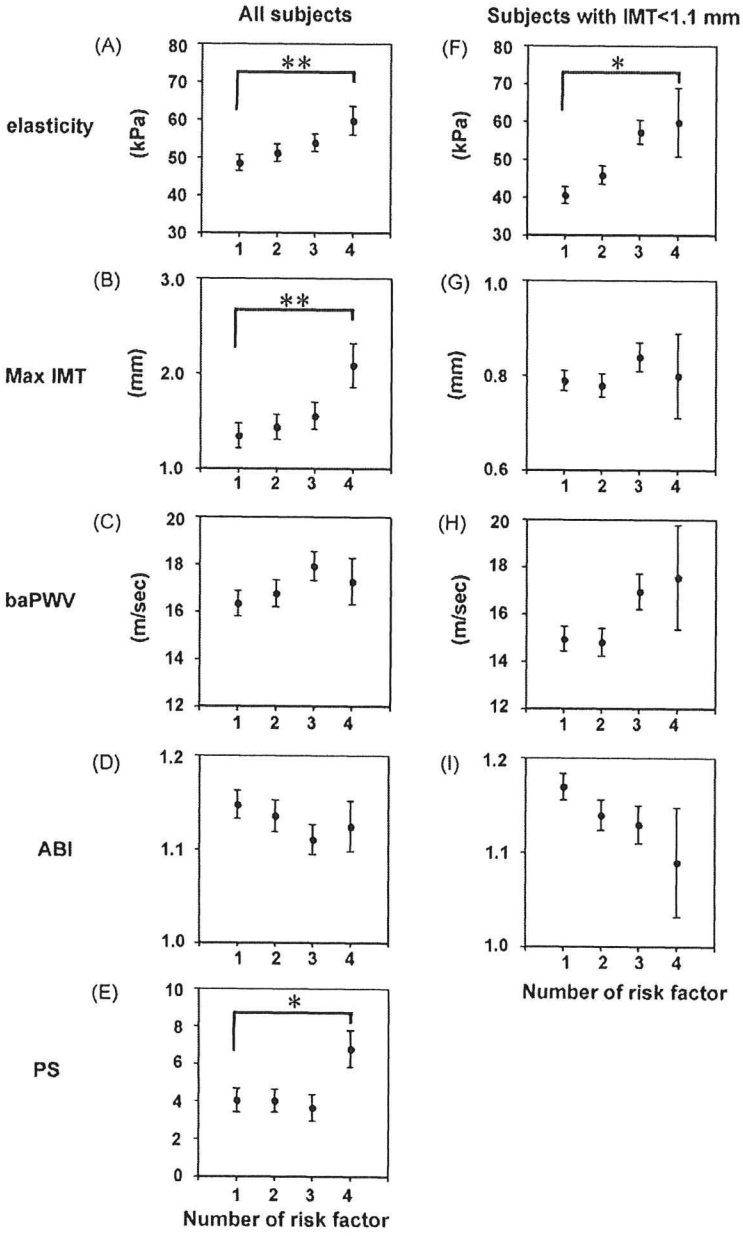

Fig. 3. Correlations of values reflecting atherosclerosis with the number of risk factors in all study subjects (A–E, $n=242$) and subjects with max IMT <1.1 mm (F–I, $n=82$). Data are presented as means ± S.E. $^{*}p<0.05$, $^{**}p<0.01$.

were taken into account in this study. All subjects had at least one risk factor, diabetes. When all the subjects were analyzed by ANCOVA, adjusted with age as a covariate, the higher the number of risk factors, the greater the attenuation of arterial elasticity values, max IMT and the plaque score (Fig. 3A, B, E). However, very interestingly, when subjects with max IMT <1.1 mm, who are regarded as not having atherosclerosis based on IMT criteria, were analyzed ($n = 82$), only age-adjusted carotid artery elasticity correlated with an increasing number of risk factors (Fig. 3F). Other age-adjusted parameters for evaluating atherosclerosis, max IMT, baPWV and ABI, showed no significant correlations with a greater number of risk factors in subjects with max IMT <1.1 mm (Fig. 3G–I).

4. Discussions

Our most important finding is that in subjects with max IMT <1.1 mm, who are regarded as being free of atherosclerosis based on IMT criteria [22,23], only carotid artery elasticity as measured with our novel non-invasive method correlated with an increasing number of risk factors. No other values obtained with the currently available methods showed correlations with the number of risk factors in these "non-atherosclerotic" subjects. Thus, our novel method of measuring arterial wall elasticity raises the possibility of detecting atherosclerosis in its early stage.

Carotid artery elasticity correlates well with results obtained with currently established methods for evaluating atherosclerosis in subjects with type 2 diabetes. These results strongly suggest that elasticity as measured with our current method reflects the severity of atherosclerosis. The measurement procedures are relatively simple, essentially the same as those of B-mode ultrasonography. In addition, arterial wall elasticity is shown as a color coded cross-sectional image with a side by side B-mode ultrasonogram, which is very practical in the clinical setting.

This novel ultrasonic method accurately tracks the movement of the arterial wall based on both the phase and the magnitude of demodulated signals, allowing instantaneous determination of the position of an object. With this method, it is possible to accurately detect small-amplitude velocity signals, less than a few micrometers, that are superimposed on arterial wall motion due to the heartbeat. This method thus allows the elasticity, a qualitative feature, of the arterial wall to be evaluated. In addition to detecting the early stage atherosclerosis, this method may enable us to evaluate progression or regression of atherosclerosis in a much shorter time than currently available methods. This possibility is extremely interesting because a means of evaluating whether or not a treatment is effective for preventing atherosclerosis is urgently needed. It usually takes years to detect the progression or regression of atherosclerosis, while it may take only months with our present method of qualitative arterial wall measurement. For example, it may be possible to detect an improvement in response to statin treatment within a few months. Similarly, we will be able to assess the effects on atherosclerosis of altering risk factors within months. These possibilities clearly merits further study.

A variety of methods are widely used for evaluating atherosclerosis. Measuring carotid IMT with ultrasound is one of the most well-established methods because it is safe, non-invasive, reproducible and easy to perform. IMT provides quantitative information, i.e. vessel-wall thickness. Depicting changes in IMT is thus generally thought to take a long time. baPWV is also a non-invasive method, which assesses atherosclerosis, as a reflection of arterial stiffness, and the usefulness of baPWV has been reported in clinical studies [26–28]. However, the pulse wave velocity depends on the ratio of the inner radius of the artery to wall thickness, which is not related to regional elasticity. It also reportedly depends on heart rate [29].

While the elasticity average of the intima and media of the carotid artery wall was calculated and used for evaluation of atherosclerosis in this study, another interesting aspect of elasticity is its distribution. The elasticity distribution, which is depicted in a histogram, might provide additional information regarding qualitative changes in atherosclerosis, and should be comprehensively studied in the future. In conclusion, our novel method for evaluating carotid artery wall elasticity holds promise for early detection of atherosclerosis.

Acknowledgments

This work was supported by a Grant-in-Aid for Scientific Research (17790599) to Y. Ishigaki and the 21st Century COE Programs "Innovative Therapeutic Development towards the Conquest of Signal Transduction Diseases" to Y. Oka from the Ministry of Education, Science, Sports and Culture of Japan. This work was also supported by a Grant-in-Aid for Research on Human Genome, Tissue Engineering (H17-genome-003) to Y. Oka. We thank Healthcare Business Company, Matsushita Electric Industrial Co., Ltd. (Panasonic), Yokohama, Japan for supplying the prototype elasticity measurement system for this study.

References

[1] Kannel WB, McGee DL. Diabetes and cardiovascular disease. The Framingham study. JAMA 1997;241:2035–8.
[2] O'Leary DH, Polak JF, Kronmal RA, et al. Carotid-artery intima and media thickness as a risk factor for myocardial infarction and stroke in older adults. Cardiovascular Health Study Collaborative Research Group. N Engl J Med 1999;340:14–22.
[3] Pignoli P, Tremoli E, Poli A, Oreste P, Paoletti R. Intimal plus medial thickness of the arterial wall: a direct measurement with ultrasound imaging. Circulation 1986;74:1399–406.
[4] Salonen JT, Korpela H, Salonen R, Nyyssonen K. Precision and reproducibility of ultrasonographic measurement of progression of common carotid artery atherosclerosis. Lancet 1993;341:1158–9.